RAPID COMMUNICATIONS IN MASS SPECTROMETRY
Rapid Commun. Mass Spectrom. 2002; **16**: 300–319

Dual parallel electrospray ionization and atmospheric pressure chemical ionization mass spectrometry (MS), MS/MS and MS/MS/MS for the analysis of triacylglycerols and triacylglycerol oxidation products

Wm. Craig Byrdwell[1]* and William E. Neff[2]

[1]Department of Chemistry and Biochemistry, Florida Atlantic University, 777 Glades Road, Boca Raton, FL 33431, USA
[2]National Center for Agricultural Utilization Research, ARS, USDA, 1815 N. University St., Peoria, IL 61604, USA

Received 22 October 2001; Revised 4 December 2001; Accepted 6 December 2001

Two mass spectrometers, in parallel, were employed simultaneously for analysis of triacylglycerols in canola oil, for analysis of triolein oxidation products, and for analysis of triacylglycerol positional isomers separated using reversed-phase high-performance liquid chromatography. A triple quadrupole mass spectrometer was interfaced via an atmospheric pressure chemical ionization (APCI) interface to two reversed-phase liquid chromatographic columns in series. An ion trap mass spectrometer was coupled to the same two columns using an electrospray ionization (ESI) interface, with ammonium formate added as electrolyte. Electrospray ionization mass spectrometry (ESI-MS) under these conditions produced abundant ammonium adduct ions from triacylglycerols, which were then fragmented to produce MS/MS spectra and then fragmented further to produce MS/MS/MS spectra. ESI-MS/MS of the ammoniated adduct ions gave product ion mass spectra which were similar to mass spectra obtained by APCI-MS. ESI-MS/MS produced diacylglycerol fragment ions, and additional fragmentation (MS/MS/MS) produced $[RCO]^+$ (acylium) ions, $[RCOO + 58]^+$ ions, and other related ions which allowed assignment of individual acyl chain identities. APCI-MS of triacylglycerol oxidation products produced spectra like those reported previously using APCI-MS. APCI-MS/MS produced ions related to individual fatty acid chains. ESI-MS of triacylglycerol oxidation products produced abundant ammonium adduct ions, even for those molecules which previously produced little or no intact molecular ions under APCI-MS conditions. Fragmentation (MS/MS) of the $[M + NH_4]^+$ ions produced results similar to those obtained by APCI-MS. Further fragmentation (MS/MS/MS) of the diacylglycerol fragments of oxidation products provided information on the oxidized individual fatty acyl chains. ESI-MS and APCI-MS were found to be complementary techniques, which together contributed to a better understanding of the identities of the products formed by oxidation of triacylglycerols.

Since the first report of atmospheric pressure chemical ionization mass spectrometry (APCI-MS) as a detector for the reversed-phase high-performance liquid chromatographic (RP-HPLC) separation of triacylglycerols (TAGs),[1] APCI-MS has become increasingly popular for analysis of TAGs. Two reasons for its popularity are that (i) it is one of the few ionization techniques that is easily interfaced to existing high performance liquid chromatography (HPLC) separation methodologies, and (ii) it is capable of producing structurally definitive ions from this class of large, neutral molecules. APCI-MS of normal triacylglycerols produces mostly protonated molecules and diacylglycerol (DAG) fragment ions, with the proportions of these being dependent on the degree of unsaturation within the TAG. This dependence of fragment ratios on unsaturation had distinct implications for the quantitation of TAGs.[2,3] Furthermore, the abundance ratios of the diacylglycerol fragments have been shown to depend on the positional placement of the fatty acyl chains on the glycerol backbone, and have been demonstrated to be useful for qualitative identification of positional isomers.[4–6] APCI-MS has also been shown to produce protonated molecules, diacylglycerol fragment ions, and diagnostically important fragment ions from TAG oxidation products (TAGOX).[7–9] Different TAGOX functional groups give different fragmentation patterns, and many of these have been characterized thus far. Applications of APCI-MS to normal TAG and TAGOX have been recently reviewed.[10]

The increasing number of reports in which authors have utilized APCI-MS for triacylglycerol analysis demonstrates that this technique has been found to be a useful and valuable tool for analysis of these large, neutral molecules.

**Correspondence to*: W. C. Byrdwell, Department of Chemistry and Biochemistry, Florida Atlantic University, 777 Glades Road, Boca Raton, FL 33431, USA.
E-mail: byrdwell@fau.edu

DOI:10.1002/rcm.581

However, there are shortcomings that keep this technique from being the one, single ideal method for lipid analysis. The first shortcoming is the lack of substantial abundances of protonated molecules obtained from highly saturated species. This lack of protonated molecules means that molecular weight information is often not directly available from saturated species. Of course, chromatographic information along with the DAG fragments has allowed their identification. Still, it is preferable to obtain abundant molecular weight information directly. Manninen and Laakso[11] showed a comparison of reagents that could be added to the sheath gas to promote molecular adduct ion formation. They reported that when the sheath gas was bubbled through an ammonium hydroxide solution, abundant $[M + 18]^+$ ammonium adducts were formed, even from highly saturated TAGs. Mochida *et al.*[12] similarly reported an increase in the percentage of $[M + NH_4]^+$ ions formed from oleic acid hydroperoxide methyl esters upon addition of ammonia to the mobile phase. Byrdwell[13] has also reported an increase in molecular adduct ion formation from TAGs brought about by incorporation of ammonium hydroxide into the HPLC mobile phase. Nevertheless, unless special steps are taken, the paucity of protonated molecules produced by saturated TAGs under APCI conditions represents a potential drawback of this technique.

Another characteristic of APCI-MS that has caused problems in the interpretation of APCI mass spectra is the lack of intact protonated molecules produced from some oxygen functional group containing TAGs. Hydroxy-containing fatty acid (FA) amide derivatives were reported by Ikeda and Kusaka[14] to readily lose the hydroxyl group by dehydration. We have previously shown that hydroxy-containing TAGs from specialty seed oils produce very small abundances of protonated molecules.[15] Instead, the hydroxyl groups were readily lost through multiple dehydrations to form $[M - nH_2O + H]^+$ fragment ions. However, a reproducible family of adducts was formed from the acetonitrile mobile phase in combination with atmospheric nitrogen, so that molecular weights could be assigned.

Loss of a hydroxyl group from an intact diacylglycerol to form a DAG fragment ion was shown in a recent report by Mu *et al.*[16] On the other hand, Adas *et al.* were able to observe peaks from large deprotonated molecules of intact hydroxy fatty acids in negative ion mode.[17] Because of their free carboxylic acid group, FAs readily formed $[M - H]^+$ ions. As a consequence, intact hydroxy-FAs were more readily observed by negative ion APCI-MS than hydroxy-TAGs have been. Overall, hydroxy-containing TAGs, DAGs, and FAs represent a challenge for analysis by APCI due to the low abundances of $[M + H]^+$ ions formed in positive ion mode.

Similarly, TAGs containing a hydroperoxide group produce virtually no protonated molecules. Kusaka *et al.*[18] showed that *rac*-1-stearoyl-2-oleoyl-3-linoleoyl-*sn*-glycerol hydroperoxides formed mostly fragments produced by loss of H_2O, $[M - H_2O + H]^+$, or by loss of the entire hydroperoxide group, $[M - H_2O_2 + H]^+$ (note that the structures shown for DAG fragment ions therein[18] erroneously show the glycerol hydroxyl group intact). Similar results for hydroperoxy TAGs have been shown by Neff and Byrdwell[7] and Byrdwell and Neff[8,9] for oxidation products produced by autoxidation[7,9] or by heated oxidation.[8] The lack of $[M + H]^+$ ions from some of these classes of oxidation products makes interpretation of complex APCI mass spectra more difficult.

Nevertheless, the rich fragmentation patterns produced by APCI-MS can prove invaluable for differentiation of classes of oxidation products, and for localizing functional groups within these products. The fragmentation patterns of epoxides, for instance, allow facile identification of this class of products, and provide a wealth of information as to the locations of the epoxide groups present. Also, the fragmentation patterns produced from the hydroperoxides are tremendously valuable in determining the identities of the multiple isobaric isomers that are present. So, the fragmentation produced by APCI-MS can on the one hand be seen as a virtue, while on the other it sometimes acts as a drawback. It would be ideal to have available an abundant intact protonated molecule, or other adduct ion, along with the rich fragmentation pattern to allow both molecular weight and structural information to be obtained from the data.

One approach that has been taken to overcome the excessive fragmentation sometimes observed during APCI-MS has been to perform electrospray ionization (ESI) instead of APCI. While it may seem counter-intuitive that neutral molecules such as TAGs could be easily ionized by ESI, methods have been found which can accomplish exactly that. As early as 10 years ago, Duffin *et al.*[19] reported ESI-MS of an unseparated mixture of TAGs dissolved in choroform/methanol (70:30). They reported ammonium and sodium adducts (from ammonium acetate or sodium acetate) of TAG mixtures infused directly into the ESI interface. Several years after that initial report, the use of ESI-MS for TAG and TAGOX started to become more widespread. Myher *et al.*[20] reported the stereospecific analysis of TAGs as their dinitrophenylurethane derivatives. Sandra *et al.*[21] reported the use of capillary electrochromatography (CEC) with ESI-MS for separation and identification of TAGs in vegetable oils. In their report,[21] ammoniated adducts were formed by addition of ammonium acetate to the mobile phase. Sjovall *et al.*[22] reported the application of ESI-MS to analysis of synthetic oxoacylglycerols (hydroperoxides, epoxides, aldehydes and alcohols). TAGs and oxidized TAGs were identified as ammoniated or sodiated adducts in positive ion mode, while deprotonated 2,4-dinitrophenylhydrazine derivatives of aldehydes were identified in negative ion mode. Cheng *et al.*[23] reported the structural analysis of triacylglycerols by infusion. Ammoniated and alkali metal (Li, Na, Cs) ions were formed, followed by collisionally activated dissociation of the precursor ions. This allowed characterization of the positions of the double bonds in the acyl chains, as well as the positions of the acyl chains on the backbone. Schuyl *et al.*[24] identified TAGs using ESI-MS after separation using argentation (silver ion) chromatography. Hsu and Turk[25] characterized TAGs as lithiated adducts (from lithium acetate) in unseparated mixtures infused into a tandem mass spectrometer. Lithiated adducts have also been used by Han *et al.*,[26] and more recently by Han and Gross,[27] for identification of TAGs in biological extracts. Dermaux *et al.*[28] analyzed fractions that were produced by supercritical

RCM

fluid chromatography, followed by capillary electrochromatography, followed by ESI-MS (with ammonium acetate) of infused CEC fractions. Steenhorst-Slikkerveer *et al.*[29] used normal-phase HPLC followed by ESI-MS to identify lipid oxidation products in vegetable oils as their sodiated adducts (from sodium iodide). Recently, ammonium adducts of diacylglycerol ethers were analyzed by Endo *et al.*[30] using reversed-phase HPLC followed by ESI with time-of-flight mass spectrometry. Hvattum[31] recently reported the use of reversed-phase HPLC coupled to ESI-MS for analysis of TAG standards.

From the number of reports of the use of ESI-MS for analysis of TAGs, TAG oxidation products, and other neutral TAG-related molecules, it is clear that ESI-MS represents a viable alternative for neutral lipid analysis. In all of these publications, an adduct of some type was formed to produce positive ions suitable for ESI-MS analysis. Ammonium adducts formed by addition of ammonium acetate were the most common adducts of choice, although alkali metals were also routinely used.

As mentioned, APCI and ESI both have benefits for TAG structural analysis. It would seem, therefore, valuable to acquire both types of data, especially for complex mixtures such as those produced during oxidation of TAGs. However, it is inconvenient to switch ionization interfaces and rerun samples sequentially using the two different ionization techniques. Running the same samples sequentially requires twice the amount of time (typical runs take 99 min), twice the amount of solvent, twice the amount of sample, and causes twice the amount of wear on columns, pumps and equipment. Although retention times are ideally identical from run to run, in practice, small differences in retention times between runs can lead to uncertainty when comparing data from a chromatographic run using one ionization method to data from a separate chromatographic run using a different ionization mode. It would be best if data from both of these complementary ionization methods could be obtained at the same time. Byrdwell[13] reported a method for obtaining data from APCI and ESI mass spectrometry techniques simultaneously from one liquid chromatographic effluent. Two mass spectrometers were employed in parallel: a single quadrupole instrument employing an APCI interface in parallel with a tandem mass spectrometer utilizing an ESI interface. The tandem mass spectrometer automatically performed alternating MS and MS/MS scans. Very shortly after this report, Siegel *et al.*[32] reported another approach to obtaining APCI and ESI MS data, for flow injection analysis of samples. They constructed an interface capable of alternating quickly between APCI and ESI modes. The approach involved providing two separate voltage sources, one for the ESI needle and one for the APCI corona needle, and changing the way the nebulizer gas (or sheath gas) was delivered. The heated vaporizer tube (used to desolvate the eluant in many APCI source designs) was removed and replaced with a coil to preheat the nebulizer gas before it nebulized the effluent. Changing temperatures between optimized APCI and ESI modes required a 30-s delay. The voltage supplies could be operated in an alternating fashion, or could be used together, to produce a mixed APCI/ESI mode.

The dual parallel mass spectrometer approach employed by Byrdwell[13] required the presence of two separate mass spectrometer systems. However, the commercially available ionization interfaces were utilized without modification to obtain the desired data. The parameters for each mass spectrometer could be optimized and maintained independently. The dual ionization source employed by Siegel *et al.*[32] could be implemented with only one mass spectrometer, but required the construction of the dual interface. Compromise conditions intermediate between the APCI and ESI optimum conditions were employed. Thus, both approaches offer the option for obtaining both APCI and ESI data from one sample (it is assumed the method demonstrated by Siegel *et al.*[32] would operate equally well with a liquid chromatographic separation as it did for infusion). In either of these two approaches the vast amount of data produced by a single chromatographic run is tremendously valuable and well worth the effort of implementing such an approach. To demonstrate this, we report here the improvement of our initial dual parallel mass spectrometer technique to allow identification of triacylglycerols and triacylglycerol oxidation products using APCI- and ESI-MS techniques, in parallel. Our previous report[13] using dual parallel mass spectrometers showed APCI-MS and ESI-MS/MS. Here we report simultaneous acquisition of APCI-MS/MS and ESI-MS/MS/MS data. A tandem mass spectrometer equipped with an APCI interface and an ion trap mass spectrometer fitted with an ESI interface were both used as detectors from the same reversed-phase chromatographic separation. In addition, an evaporative light scattering detector (ELSD) was used, providing a total of three detectors, overall.

MATERIALS AND METHODS

Materials

Commercially available canola oil was purchased from a local market. Synthetic triolein (99+ % purity) was purchased from NuCheck Prep (Elysian, MN, USA). Heated oxidation was performed as previously described.[8] Briefly, 5 g of the TAG was placed in 12.5 × 2.0 cm test tube and heated to 190 °C by submersion in a temperature-controlled silicone oil bath. The samples used for this report were oxidized for 6 h.

TAG positional isomers were purchased from Sigma Chemical Co. (St. Louis, MO, USA). Two mixtures were made, one containing 1,3 positional isomers (OPO and POP), and one containing 1,2 positional isomers (OOP, PPO and OOS). These TAG positional isomers were dissolved in dichloromethane and run by the same HPLC method as the normal canola oil. Acetonitrile (ACN) and dichloromethane (DCM) purchased from Sigma Chemical Co. (St. Louis, MO, USA) were HPLC grade and were used without further purification.

Liquid chromatography

Non-aqueous reversed-phase high-performance liquid chromatography (RP-HPLC) was performed using an LDC 4100 quaternary pump (Thermo Separation Products, Schaumburg, IL, USA) with a membrane degasser. Two Inertsil ODS-3 columns, 25 cm × 4.6 mm, 5 μm (MetaChem

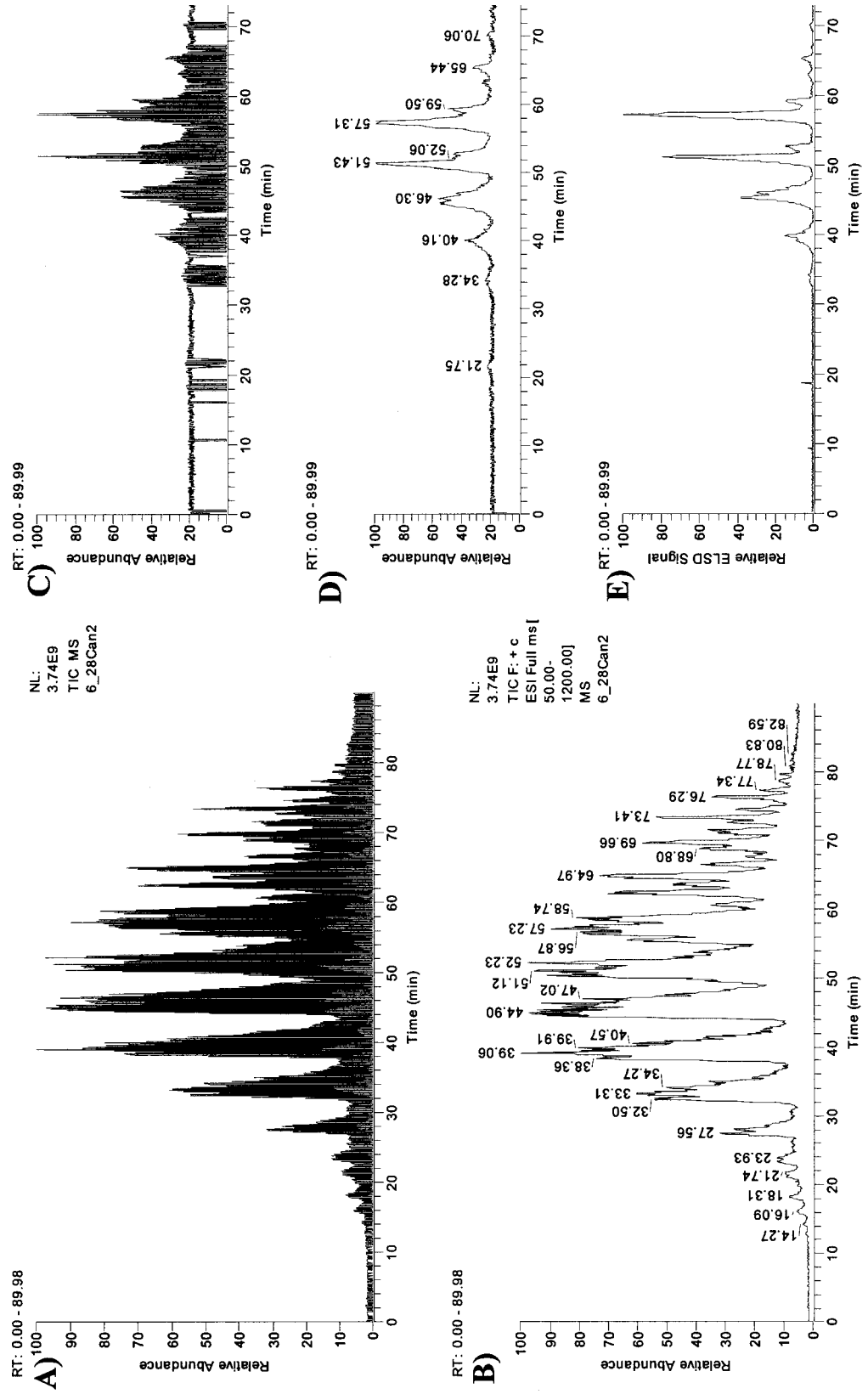

Figure 1. Electrospray ionization (ESI) mass spectrometry (MS) and atmospheric pressure chemical ionization (APCI) MS chromatograms of normal canola oil obtained simultaneously using dual parallel mass spectrometers. (A) Total ion chromatogram obtained by ESI-MS; (B) ESI-MS chromatogram filtered to show only full MS scans; (C) APCI-MS total ion chromatogram; (D) APCI-MS chromatogram filtered to show only full MS scans; (E) Evaporative light scattering detector (ELSD) chromatogram.

RCM

Technologies), in series were used. The gradient program used for the separation of the canola oil was as follows: initial-DCM/ACN (30:70), held for 20 min; linear from 20 to 40 min to DCM/ACN (40:60), held for 10 min; linear from 50 to 70 min to DCM/ACN (60:40), held for 5 min; linear from 75 to 80 min to DCM/ACN (70:30), held for 5 min; recycled to original conditions from 85 to 99 min. The flow rate used for this separation was 0.7 mL/min. The gradient program used for the separation of the oxidation products was as follows: initial-DCM/ACN (25:75), held for 20 min; linear from 20 to 50 min to DCM/ACN (30:70); linear from 50 to 85 min to DCM/ACN (70:30); recycled to original conditions from 85 to 99 min. The flow rate used for this separation was 0.8 mL/min. The effluent from the two columns in series was split by using two Valco Tees in series. 0.005 in. i.d. tubing was connected from the 90° exit of the first tee to the evaporative light scattering detector (ELSD), while the straight-through exit of the tee was connected to the second tee via a 4-cm piece of 0.005 in. i.d. stainless tubing. To both of the outlets of the second tee were connected equal lengths (3 ft) of 0.1 mm (= 0.0039 in) i.d. deactivated fused-silica capillary tubing, attached via an adapting ferrule. One capillary was attached to the APCI interface and the other was attached to the ESI interface. The ELSD was a model ELSD MKIII (Varex, Burtonsville, MD, USA). The drift tube was set to 140 °C, and the nebulizer gas (high purity N_2) was set to 2.0 standard liters per minute and a pressure of 26.6 psi. The ELSD signal was connected to the user interface of the tandem mass spectrometer for data acquisition.

Mass spectrometry

A Finnigan MAT TSQ 700 (ThermoFinnigan, Inc., San Jose, CA, USA) was used for acquisition of APCI-MS data. The TSQ700 gave optimal signal in Q3 low mass mode. For full scans using Q3, Q1 was used in RF-only mode. The vaporizer heater was operated at 400 °C, with the heated capillary set to 265 °C. The corona current was set to 6.0 μA. Sheath and auxiliary gases were set to 35 psi and 5 mL/min, respectively. The sheath gas was bubbled through methanol (~400 mL) in a 1-L bottle prior to entry into the ionization source. Spectra of normal TAGs were obtained from *m/z* 150–1200 with a scan time of 1.0 s. Spectra of TAGOX were obtained from *m/z* 150–1200 with a scan time of 1.0 s until 50 min, and thereafter the scan range was from *m/z* 150–1950 with a scan time of 2.0 s. The scan range and time were automatically changed using a time-dependent instrument command language (ICL) procedure. The parameters of the ICL programs have been previously described.[13] Additional procedures were written for the TAGOX to allow the change in scan range at 50 min. All parameters were optimized for TAG analysis. The parent quadrupole (Q1) offset was −5.0 V, the collision cell (Q2) offset was −5.0 V in full scan mode and −25.0 V in MS/MS mode, and the product quadrupole (Q3) offset was −5.0 V. The 'msms correction factor' was 5% throughout. Argon was used as the collision-induced dissociation (CID) gas. Four scans were obtained in full scan mode, then the CID gas was turned on and four MS/MS scans of each of the two most abundant precursor ions were collected.

An LCQ Deca (ThermoFinnigan, Inc., San Jose, CA, USA) ion trap mass spectrometer was used for acquisition of ESI-MS data. Scans were obtained from *m/z* 50–1200, in centroided positive ion mode for normal TAG. For TAGOX, scans were obtained from *m/z* 50–1200 up to 50 min, and from *m/z* 50–2000 thereafter. The ion trap was set to automatically select the most abundant precursor ion and perform MS/MS, and then to select the most abundant first-generation product ion and perform MS/MS/MS. The activation energy was 58% (arbitrary units) with a 'q factor' of 0.25. The activation time was 900 ms. For all separations, 20 mM ammonium formate solution in H_2O/ACN (1:4) was added as a sheath liquid from an AB 140B syringe pump (Applied Biosystems, Foster City, CA, USA) at a flow rate of 20 μL/min. The ammonium formate electrolyte solution was prepared as follows: 100 mM ammonium formate solution in deionized water was prepared and diluted 1:4 with ACN.

RESULTS AND DISCUSSION

Normal canola oil

ESI-MS and APCI-MS spectra

Figure 1 shows the chromatograms obtained by ESI-MS, APCI-MS and ELSD detectors for normal (unoxidized) canola oil. The ELSD chromatogram was acquired to provide performance verification on the TSQ mass spectrometer, and will be discussed only briefly. The total ion chromatograms (TICs) are shown, along with TIC that have been filtered to show only full scans (no MS/MS or MS^3). The data obtained using the older ICIS™ software of the TSQ were imported into the Xcalibur™ software on the LCQ to allow the chromatograms and spectra to be more easily compared. Note that the chromatographic peaks were sufficiently broad (especially for polyunsaturated species) that the retention times of the local maxima which were labeled by the software were close but not identical, even though the peaks did elute at the same times on both mass spectrometers (the distances from the splitting tee at the end of the column to the ionization sources were identical, as was the diameter of the capillary tubing used).

The chromatograms obtained by APCI-MS in MS mode were very similar to those reported previously.[33] The mass spectra of TAGs obtained by APCI-MS exhibited all of the features previously reported for these spectra. The TAGs with less than three sites of unsaturation produced DAG fragment ions as base peaks in their mass spectra, those with three or four sites produced either a DAG or a protonated TAG base peak, and TAGs with more than four sites of unsaturation produced a protonated molecule as base peak. Typical mass spectra obtained by ESI-MS and APCI-MS are shown in Fig. 2. One difference between these runs and those performed previously was that here the sheath gas was bubbled through methanol. LC/APCI-MS chromatograms of canola oil performed using the LCQ ion trap mass spectrometer (data not shown) exhibited much more extensive adduct formation (formed from solvent vapor and atmospheric gases, as in Ref. 15) than had previously been observed using the TSQ 700 mass spectrometer; this is believed to be due to the larger diameter of the heated capillary incorporated into the LCQ Deca design. Sparging the sheath gas through methanol virtually completely

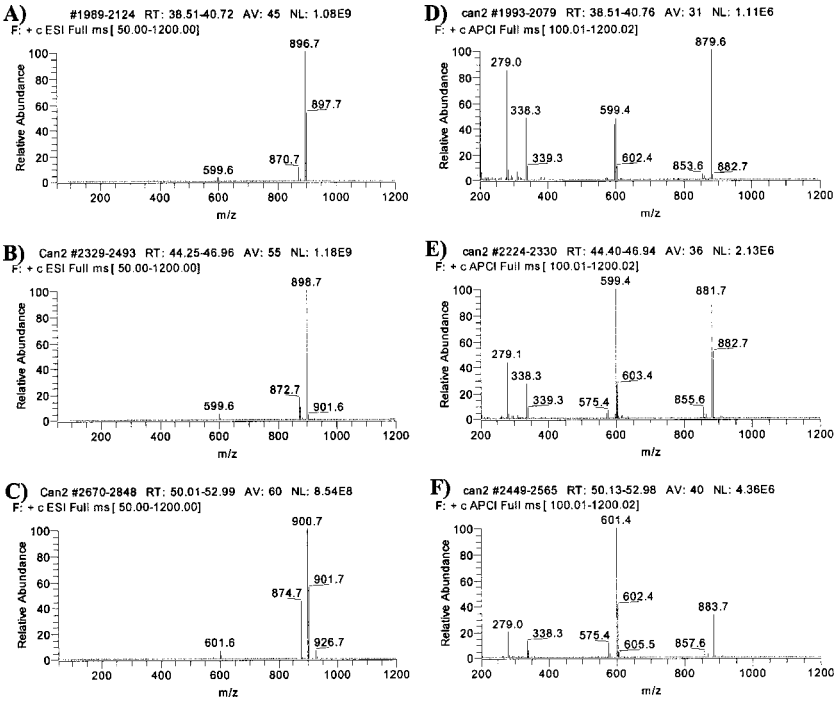

Figure 2. ESI-MS and APCI-MS spectra of canola oil triacylglycerols. (A) ESI-MS spectrum of ammoniated LLL; (B) ESI-MS spectrum of ammoniated LLO; (C) ESI-MS spectrum of ammoniated OOL; (D) APCI-MS spectrum of LLL; (E) APCI-MS spectrum of LLO; (F) APCI-MS spectrum of OOL. See abbreviations in Fig. 3.

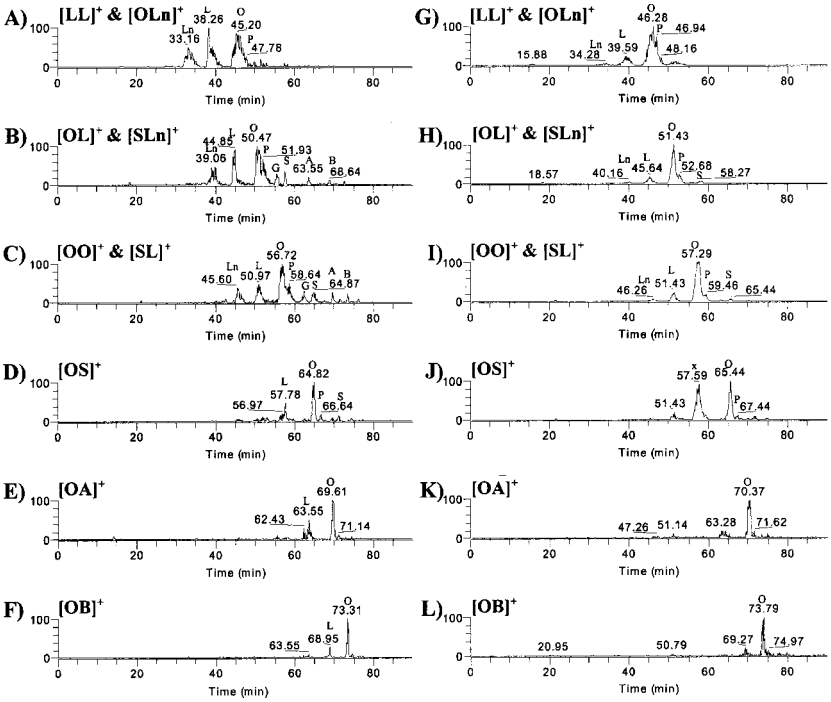

Figure 3. Extracted ion chromatograms of diacylglycerol fragment ions obtained by ESI-MS (A–F) and by APCI-MS (G–L). (A) $[LL]^+$ or $[OLn]^+$; (B) $[OL]^+$ or $[SLn]^+$; (C) $[OO]^+$ or $[SL]^+$; (D) $[OS]^+$; (E) $[OA]^+$; (F) $[OB]^+$; (G) $[LL]^+$ or $[OLn]^+$; (H) $[OL]^+$ or $[SLn]^+$; (I) $[OO]^+$ or $[SL]^+$; (J) $[OS]^+$; (K) $[OA]^+$; (L) $[OB]^+$. Fatty acid abbreviations: S = stearic (18:0), O = oleic (18:1), L = linoleic (18:2), Ln = linolenic (18:3), A = arachidic (20:0), G = gadoleic (20:1), B = behenic (22:0).

RCM

eliminated these undesirable adducts, and resulted in much cleaner mass spectra. Based on this observation, we chose to incorporate methanol sparging into all APCI runs using both the LCQ and the TSQ. However, this did affect the sensitivity of the TSQ, giving a slightly diminished signal. The spectra obtained by APCI-MS using the TSQ 700 did not exhibit troublesome levels of adduct formation under normal conditions, so sparging with methanol was completely optional on this machine. However, we found sparging to be absolutely necessary for APCI-MS on the LCQ Deca.

The ESI-MS analyses performed using the LCQ Deca produced mass spectra with abundant ammoniated adduct ions for all species. The ESI-MS spectra shown in Figs 2(A)–(C) exhibit mainly ammoniated molecules, with no $[M + H]^+$ observed. All of the ions in the high mass region of the mass spectra represented TAG molecular species. No appreciable amounts of other molecular adduct ions were present. For example, in the spectrum for LLL (Fig. 2(A)), which had an $[M + NH_4]^+$ ion at *m/z* 896.7, one can see a peak arising from PLLn, at *m/z* 870.7, which eluted with a similar retention time. Under APCI-MS conditions, LLL exhibited an $[M + H]^+$ at *m/z* 879.6, as shown in Fig. 2(D), while PLLn exhibited an $[M + H]^+$ at *m/z* 853.6 In the ESI-MS spectra, small abundances of diacylglycerol fragment ions (formed from loss of one fatty acyl chain) were evident. The abundances of these DAG fragment ions were much less than were observed in APCI-MS spectra. Previously, DAG fragment ions have proved to be very important in identification of TAG molecular species. The complementary nature of ESI-MS spectra compared to APCI-MS spectra is readily apparent in Fig. 2. The abundances of DAG fragment ions in ESI-MS spectra could be increased by employing 'up-front collision induced dissociation' in the ESI interface region (data not shown). The APCI-MS spectra (e.g. Figs 2(D)–(F)) contained ubiquitious background ions at *m/z* 279 and 338 that were observed to have arisen as the vaporizer heater aged and retained contamination that was not removed with cleaning.

In our previous reports, the patterns observed in extracted ion chromatograms (EICs) of the DAG fragment ions have been invaluable for identification of TAGs in all types of samples. Examples of EICs obtained by ESI-MS and by APCI-MS are shown in Fig. 3. In any given EIC, a peak appears for every TAG molecular species that lost a fatty acid (FA) to yield the DAG fragment. Thus, a peak appeared in the EIC for each FA that was combined with the DAG to form a TAG. The peaks corresponding to each FA, which combined with the DAG to form the TAG, are labeled in Fig. 3. Although the DAG fragments produced by ESI-MS were small, they were still present in sufficient abundance to allow EICs of the DAG fragment ions to be produced. One primary difference between the EICs obtained by ESI-MS compared to those obtained by APCI-MS was that within any particular EIC, the peaks arising from the polyunsaturated FAs (linoleic and linolenic acids) were larger than the corresponding peaks in the EICs obtained by APCI-MS. This difference arose from two factors. First, ESI-MS spectra did not exhibit the great difference in the ratios of DAG fragments to TAG molecular ions that APCI-MS spectra exhibited. It has been extensively reported previously that,

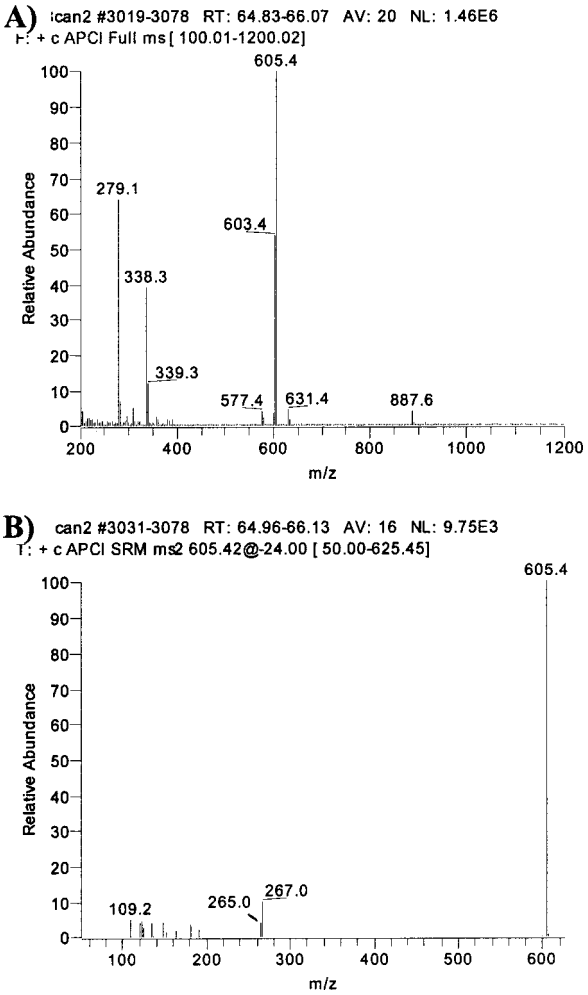

Figure 4. (A) APCI-MS spectrum of OOS; (B) APCI-MS/MS spectrum of *m/z* 605.4 Da peak, $[OS]^+$, from OOS.

under APCI-MS conditions, polyunsaturated TAGs produced lower DAG fragment abundances than more saturated species, giving more abundant $[M + H]^+$ ions, whereas less saturated TAGs gave mostly DAG fragments. Since ESI-MS did not produce the great difference in the amount of DAG fragments from saturated versus unsaturated species, the sensitivity of polyunsaturates was not less than that of more saturated species. Second, based on the sizes of the peaks arising from polyunsaturated FAs, the polyunsaturated TAGs appear to be more efficiently ionized than more saturated species. This is in agreement with the recent report by Han and Gross[27] that showed that TAGs with higher degrees of unsaturation showed higher response to ESI-MS than more saturated species. This behavior is in contrast to the behavior of TAGs under APCI-MS conditions. We have previously shown that the difference in the relative amounts of DAG versus TAG ions in APCI-MS spectra had distinct implications for quantitative analysis, and a method was previously developed to compensate for this discrimination in fragmentation behavior to allow quantitative analysis.[2,34] The data obtained by Han and Gross[27] were obtained from unseparated TAGs. Quantitative analysis of TAGs by ESI-MS with separation on a reversed-phase HPLC system will be the subject of further investigation.

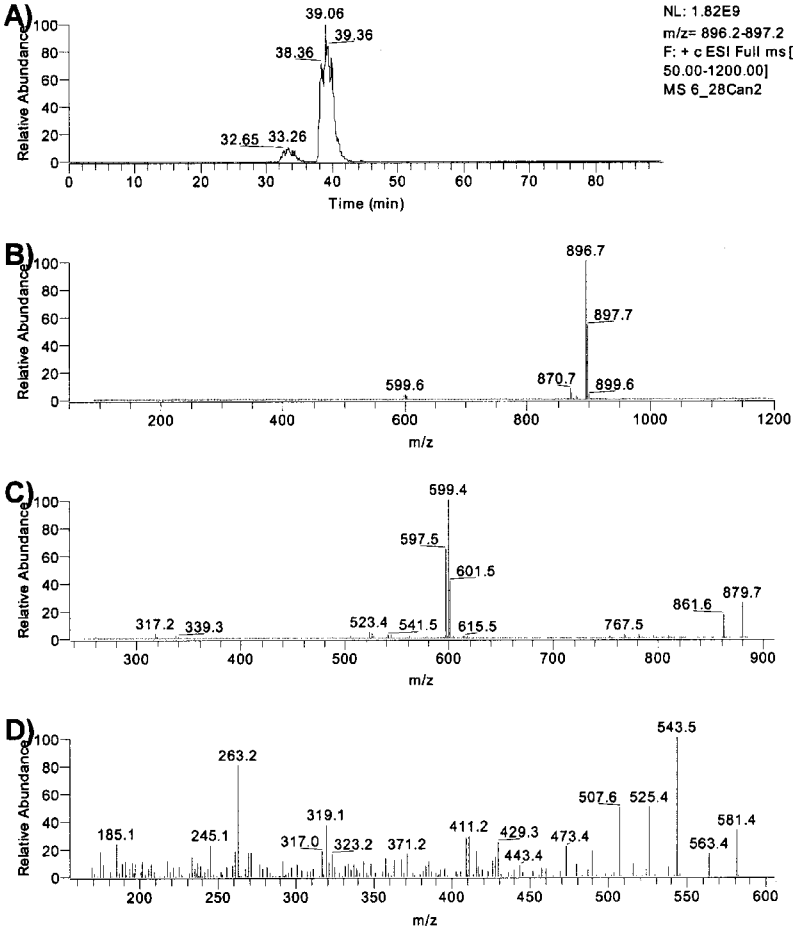

Figure 5. (A) Extracted ion chromatogram (EIC) of *m/z* 896.7 (=[LLL + NH_4]$^+$ and [OLLn + NH_4]$^+$). (B) ESI-MS spectrum of large peak in (A); (C) ESI-MS/MS spectrum of *m/z* 896.7; (D) ESI-MS/MS/MS spectrum of *m/z* 599.4 formed from *m/z* 896.7.

The ELSD chromatogram

The ELSD detector chromatogram (Fig. 1(E)) is similar to the APCI-MS TIC (Fig. 1(D)). The APCI-MS TIC chromatogram signal-to-noise ratio could be improved by including only the *m/z* ranges of the DAG and TAG ions, eliminating lower and higher ranges. The ELSD detector has been shown to give results similar to those obtained by flame ionization detection (FID).[35] Without correction factors applied to MS, such as in the case of visually comparing Fig. 1(E) to Fig. 1(D), HPLC-FID gives results with lower average error than raw APCI-MS results. However, FID has been shown to give greater error in the composition of TAG mixtures with known compositions than APCI-MS after correction using response factors.[2,34] So, the ELSD detector gives a better visual representation of the composition of the oil without more rigorous quantitative analysis applied. The response factors used for APCI-MS usually reflect larger factors for unsaturated TAGs than saturates. Saturated TAGs usually have lower response factors, or a factor of 1.00. Unsaturated TAGs are usually assigned larger response factors. An exception is linolenic acid, for which extracted ion chromatogram peaks contain a contribution from ^{13}C-isotope variants of linoleic acid-containing TAGs, as explained elsewhere.[2] In other words, by APCI-MS, TAGs with more sites of unsaturation often under-respond, compared to saturates. On the other hand, since the ELSD represents the closer approximate composition, it is apparent by comparison of Figs 1(E) and 1(B) that, by ESI-MS, polyunsaturated TAGs are over-represented, although saturates still produced abundant signals (in the form of ammoniated molecules).

As mentioned, ionization by APCI produced a greater degree of fragmentation than ionization by ESI. The fragments produced were mostly DAG fragment ions, similar to those which would be obtained from MS/MS of [M + H]$^+$. Additional fragmentation produced by MS/MS of the DAG fragments yielded second-generation fragments related to the individual acyl chains, similar to what would be obtained by MS/MS/MS of the protonated molecule. MS/MS product ion spectra of DAG fragments in the APCI mass spectra are shown in Fig. 4. To provide the maximum structural information, the range over which precursor ions were selected in the APCI mass spectra was constrained (by the ICL procedure written by us) to the DAG *m/z* range 500–700 in the canola oil analyses. The collision cell voltage was adjusted to maximize the signals in the range *m/z* 200–350. The DAG precursor ion was still quite abundant in these daughter spectra, but the smaller fragments nevertheless

RCM

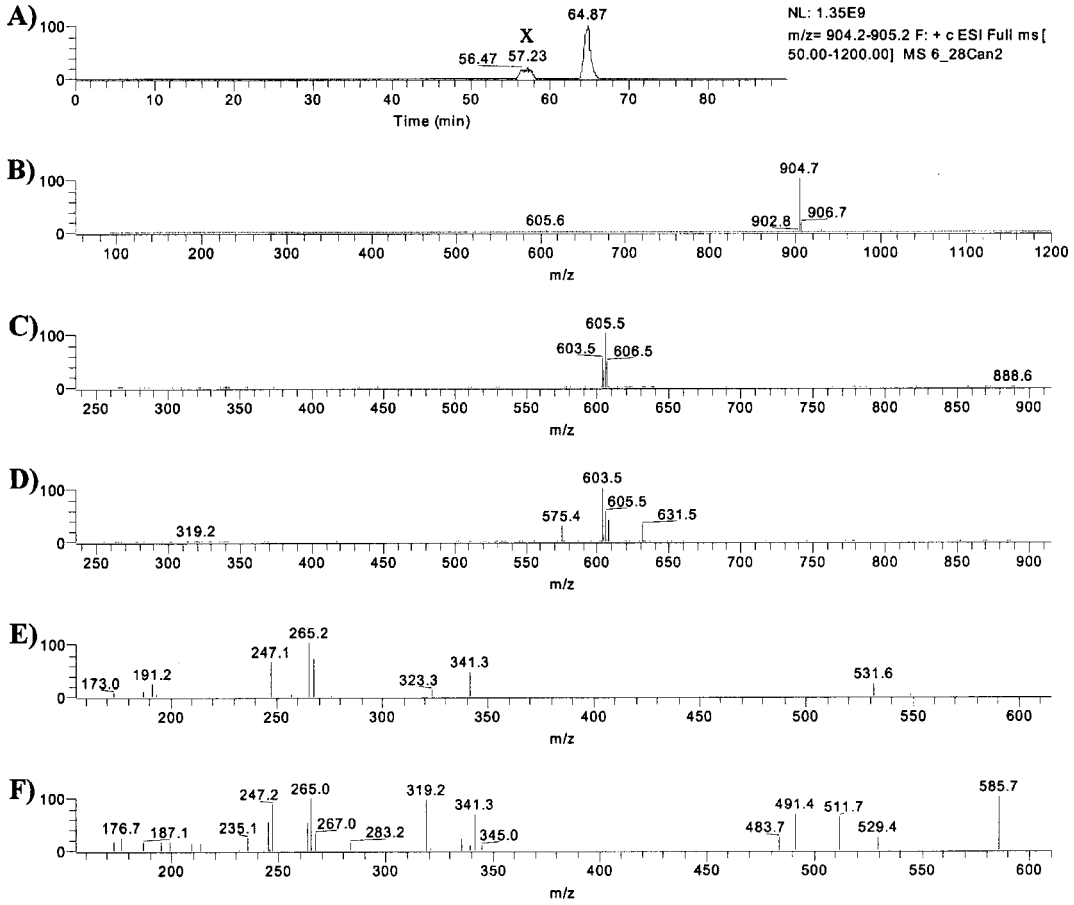

Figure 6. (A) Extracted ion chromatogram of *m/z* 904.7 (=$[OOS + NH_4]^+$, $[SLS + NH_4]^+$ and $[PLA + NH_4]^+$); (B) Average ESI-MS spectrum across peak at 64.9 min; (C) Average ESI-MS/MS spectrum of front portion of peak at 64.9 min; (D) Average ESI-MS/MS spectrum of latter portion of peak at 64.9 min; (E) Average ESI-MS/MS/MS spectrum of peak at *m/z* 605.5 in (C); (F) Average ESI-MS/MS/MS spectrum of peak at *m/z* 603.5 in (D). In (A), X represents the isotope peak from *m/z* 902.7.

were maximized. The DAG precursor ion peak could be virtually eliminated by using higher collision energies, so the ratio of the lower mass peaks to the precursor ion could thereby be increased, but the absolute abundances of smaller fragments also suffered. Four types of fragments were the most common in the MS/MS of DAG precursor ions: $[RCO]^+$, $[RCO - H_2O]^+$, $[RCOO + 58]^+$ (=$[RCO + 74]^+$) and $[RCOO + 58\text{-}H_2O]^+$. The $[RCO]^+$ and $[RCOO + 58]^+$ peaks have been commonly reported to arise from TAGs by APCI-MS,[5,6,9,16,36,37] ESI-MS,[19,23,25] and other ionization methods, dating back to the 1970s.[38–40] In addition, identical fragments arose from APCI-MS of phospholipids.[13] A list of the calculated masses of these four ions for the common 16- and 18-carbon acyl chains is given in Table 1 as a convenient aid in peak identification. In the APCI-MS/MS spectrum shown in Fig. 4(B), the $[RCO]^+$ peaks for both the stearic and oleic acid chains are apparent, which provided confirmation of the identities of the acyl chains; however, no other intact acyl chain fragments were present. In other spectra, combinations of the above fragment ions occurred to varying degrees. The APCI-MS spectra were less consistent and reproducible than the ESI-MS spectra.

MS/MS and MS/MS/MS spectra

ESI-MS, ESI-MS/MS and ESI-MS/MS/MS spectra are shown in Figs 5 and 6. Figure 5(A) shows an EIC of the

Table 1. Common acyl chain fragment ion calculated *m/z* values

	$[RCO]^+$	$[RCO - H_2O]^+$	$[RCOO + 58]^+$	$[RCOO + 58 - H_2O]^+$
P	239.24	221.23	313.27	295.26
Ln	261.22	243.21	335.26	317.25
L	263.24	245.23	337.27	319.26
O	265.25	247.24	339.29	321.28
S	267.27	249.26	341.31	323.30

Abbreviations: P—palmitic acid; Ln—linolenic acid; L—linoleic acid; O—oleic acid; S—stearic acid.

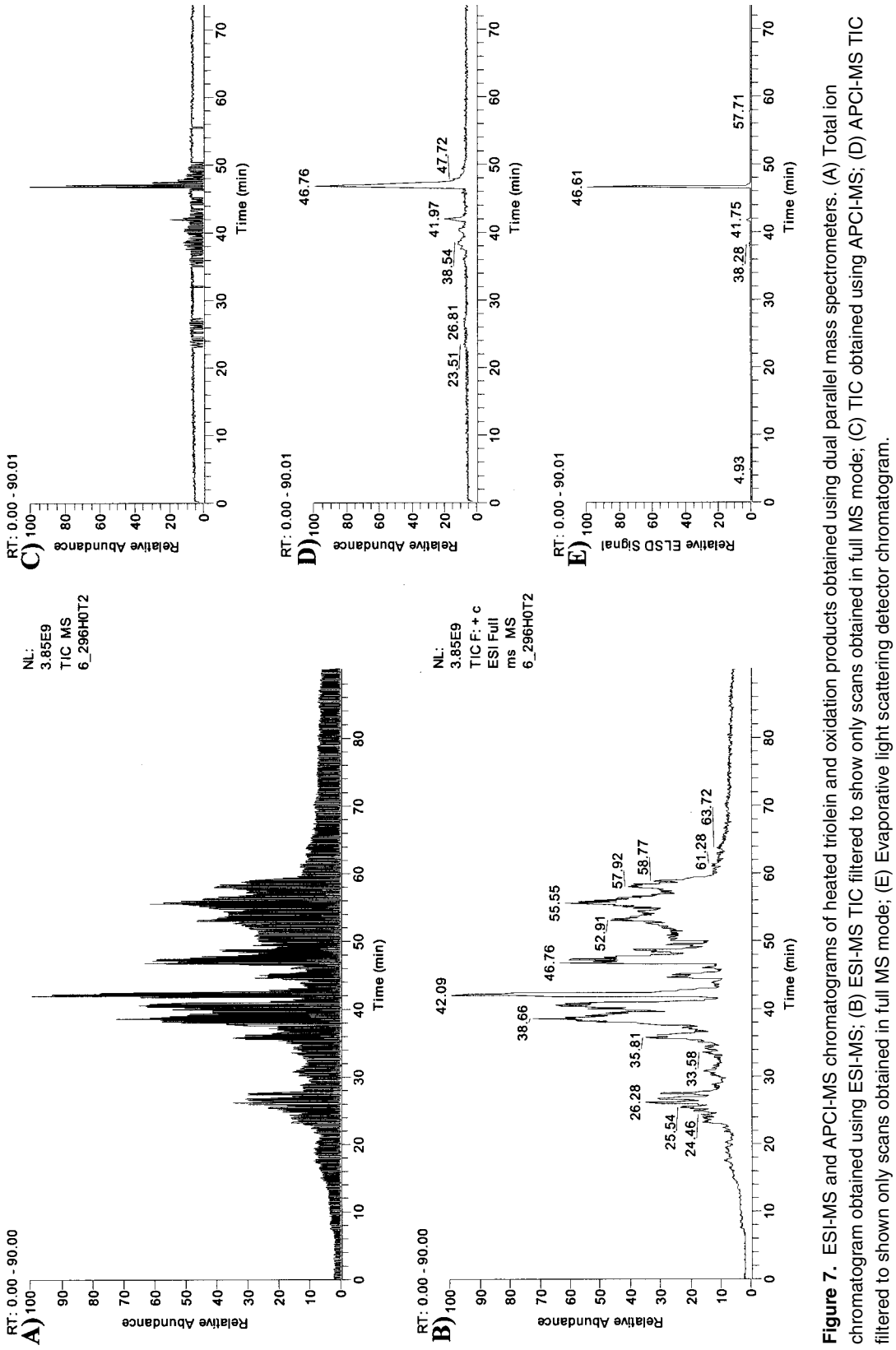

Figure 7. ESI-MS and APCI-MS chromatograms of heated triolein and oxidation products obtained using dual parallel mass spectrometers. (A) Total ion chromatogram obtained using ESI-MS; (B) ESI-MS TIC filtered to show only scans obtained in full MS mode; (C) TIC obtained using APCI-MS; (D) APCI-MS TIC filtered to shown only scans obtained in full MS mode; (E) Evaporative light scattering detector chromatogram.

RCM

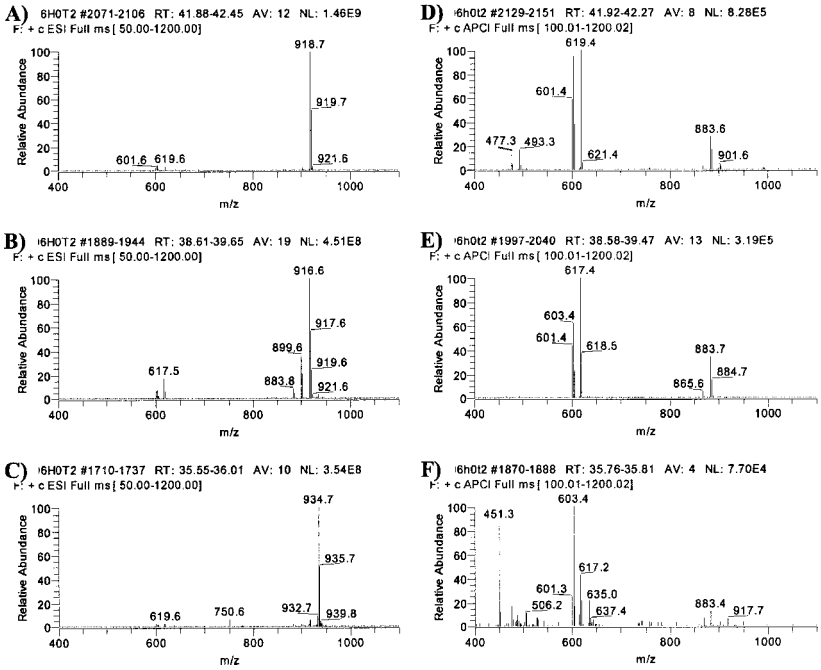

Figure 8. ESI-MS and APCI-MS spectra of triolein oxidation products. (A) ESI-MS spectrum of ammoniated OOS-epoxide; (B) ESI-MS spectrum of ammoniated OOO-epoxide; (C) ESI-MS spectrum of ammoniated OOO-hydroperoxide; (D) APCI-MS spectrum of OOS-epoxide; (E) APCI-MS spectrum of OOO-epoxide; (F) APCI-MS spectrum of OOO-hydroperoxide.

mass associated with the LLL (=OLLn) ammoniated molecule; Fig. 5(B) is a full scan mass spectrum averaged across the breadth of the largest peak in the EIC; and Fig. 5(C) is the ESI-MS/MS spectrum of the precursor at *m/z* 896.7. At high *m/z* in the MS/MS spectrum, $[M + H]^+$ and $[M + H - H_2O]^+$ ions were seen to arise from the ammoniated precursor. Three DAG fragment ions were formed, $[OL]^+$, $[LL]^+$ (=$[OLn]^+$), and $[LLn]^+$. These ions showed that both LLL and OLnL were present and contributed to the *m/z* 896.7 precursor ion. In Fig. 5(D), the ESI-MS/MS/MS spectrum of the *m/z* 599.4 precursor is seen to exhibit extensive fragmentation. Since *m/z* 599.4 could represent $[LL]^+$ or $[OLn]^+$, fragments representative of L^+, O^+, and Ln^+ were all present. One notable characteristic of ESI-MS/MS/MS spectra of polyunsaturated TAGs was the extensive charge-remote fragmentation which occurred. In contrast, the ESI-MS/MS/MS spectra of more highly saturated species showed much less extensive charge-remote fragmentation, and contained mostly the ions listed in Table 1.

Figure 6 gives examples of data showing overlapped TAG which eluted between 64 and 66 min. The EIC of *m/z* 904.7 is given in Fig. 6(A). An average mass spectrum across the large peak in this EIC is given in Fig. 6(B). The ammoniated molecule at *m/z* 904.7 indicated the possible presences of OOS, SLS, and PLA, as well as others. Mass spectral data allowed these isobaric species to be differentiated. The mass spectrum shown in Fig. 6(C) represents an average across the middle portion of the peak in the EIC in Fig. 6(A). The fragment ions at *m/z* 603.5 and 605.5 indicate the presence of $[OO]^+$ and $[OS]^+$ moieties, respectively. The lack of fragments at *m/z* 575.4, 607.5 and 631.5 indicates the absence of PLA or SLS in this portion of the chromatographic peak. The fragments and the ammoniated molecule, taken together, indicated the presence of only OOS in this part of the EIC peak. The mass spectrum in Fig. 6(D) represents an average across the later portion of the peak in the EIC in Fig. 6(A). The fragment at *m/z* 603.5 indicates the presence of $[SL]^+$ and/or $[OO]^+$; the fragment at *m/z* 605.5 indicates that some $[OS]^+$ was still present; the fragment at *m/z* 575.4 indicates the presence of $[PL]^+$; the fragment at *m/z* 631.5 indicates the presence of $[LA]^+$; and the fragment at *m/z* 607.5 indicates the presence of $[SS]^+$ and/or $[PA]^+$. Taken together, these fragments clearly indicate the presence of PLA and SLS, which eluted in the later portion of the peak in Fig. 6(A), with some OOS still present. The ESI-MS/MS/MS spectra in Figs 6(E) and 6(F) confirmed these observations. The ESI-MS/MS/MS spectrum in Fig. 6(E) showed only acyl chain fragments related to oleoyl and stearoyl fatty acyl chains. As Table 1 shows, *m/z* 265.2 represents the $[RCO]^+$ fragment from oleic acid, while *m/z* 267.2 is the $[RCO]^+$ fragment from stearic acid. Other fragments included the $[RCO - H_2O]^+$ ion for oleic acid and the $[RCOO + 58]^+$ and $[RCOO + 58\text{-}H_2O]^+$ fragments related to stearic acid.

The ESI-MS/MS/MS spectrum in Fig. 6(F) was produced by fragmentation of the peak at *m/z* 603.5 in Fig. 6(D). This spectrum shows $[RCO]^+$ peaks for stearic, oleic and linoleic acids at *m/z* 267.0, 265.0 and 263.2, respectively. These fragments indicate that the *m/z* 603.5 peak arose from both $[OO]^+$ and $[SL]^+$ in this part of the chromatographic peak. The larger number of fragments in Fig. 6(F) highlights the difference between the spectra of DAG fragment ions

containing polyunsaturated versus saturated FA. The presence of linoleic acid in the DAG precursor ion caused a higher degree of charge-remote fragmentation than occurred during the fragmentation depicted in Fig. 6(E).

Triolein oxidation products

ESI-MS and APCI-MS data

Figure 7 represents chromatograms of heated synthetic triolein and its oxidation products produced during the heating process. Comparison of Figs 7(B) and 7(D) shows that all oxidation products gave substantially higher signals by ESI-MS, relative to that of unchanged triolein (at 46.8 min), than the corresponding signal obtained by APCI-MS. High molecular weight dimers, oxidized dimers and dimer addition products, which eluted after triolein, also produced much more intense signals by ESI-MS than by APCI-MS. Figure 8 shows ESI-MS and APCI-MS spectra of some of the oxidation products that eluted before triolein. The *m/z* range displayed in these spectra was limited to show better resolution of important ions. As with normal TAGs, the ESI-MS spectra exhibited primarily ammoniated molecules, with low abundances of DAG fragment ions. As with normal TAGs, few or no other intact ionized molecules were formed by ESI-MS. The APCI-MS spectra, on the other hand, were similar to those reported previously for these compounds.[7,8] Very low-abundance $[M + H]^+$ ions were observed for the oxidation products by APCI-MS. These APCI mass spectra exhibited somewhat lower-abundance $[M + H]^+$ ions than previously reported, probably as a result of the methanol sparging which was employed here. These spectra, and the chromatograms in Fig. 7, made it apparent that ESI-MS was superior to APCI-MS for molecular weight determination of the oxidation products, especially for the hydroperoxides. However, the fragments produced by APCI-MS were quite useful and provided valuable data complementary to the ESI-MS data. For example, the fragments from OOS-epoxide (Fig. 8(D)) clearly showed the position of the epoxide functional group, as reported previously.[7,8] The diacylglycerol fragments also clearly showed the oxygen-containing diacylglycerol moieties. Thus, the dual parallel mass spectrometer arrangement provided a wealth of intact molecular adduct ions on one instrument and useful fragmentation patterns on the other, which allowed thorough characterization of the oxidation products.

High molecular weight oxidation products

The chromatograms of triolein oxidation products in Fig. 7 show dramatic differences in the responses for high molecular weight TAG oxidation products. ESI-MS provided very good response for these large molecules, but APCI-MS gave very poor response for these compounds. As we reported previously,[8] it was necessary to collect fractions and produce samples enriched in these components before suitable APCI-MS spectra could be obtained. ESI-MS spectra of high molecular weight dimers could be obtained from individual sample injections, without the need for enrichment. No usable mass spectra were obtained by APCI-MS of the non-enriched sample, and no such spectra of these components are presented here.

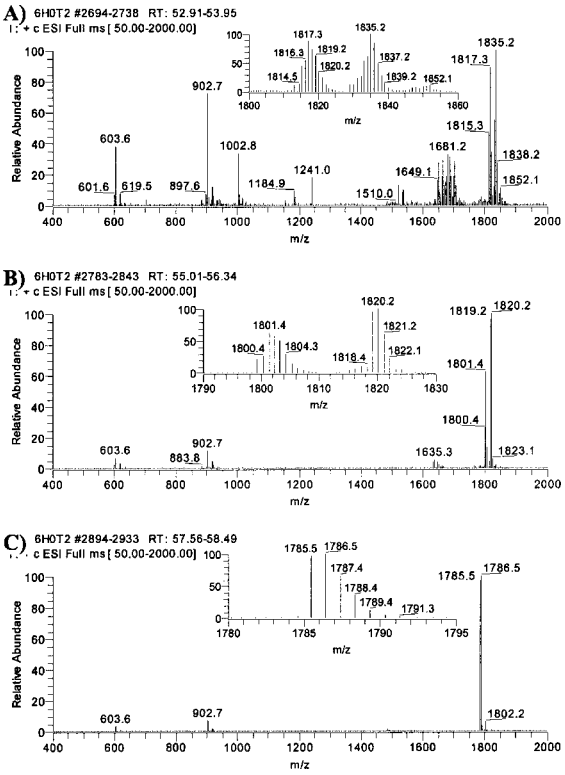

Figure 9. ESI-MS spectra of ammoniated high molecular weight (MW) oxidation products. (A) ESI-MS spectrum of peak eluted near 53.5 min; (B) ESI-MS spectrum of peak eluted near 55.5 min; (C) ESI-MS spectrum of peak eluted near 58 min. Retention times refer to Fig. 7.

Figure 9 shows ESI-MS spectra of three of the main classes of high molecular weight products, which eluted at 53–53.5, 55.5 and 58 min in Fig. 7. An inset in each frame shows an expanded view of the ammoniated molecule region. The mass spectrum of the first part of the peak that eluted at 58 min (eluted last = most non-polar) is shown in Fig. 7(C), and exhibits a distribution of *m/z* values around the calculated mass of the ammoniated dimer of triolein, minus two hydrogen atoms: $2 \times 884.8 + 18 - 2H = 1785.6$ Da. This is consistent with our previous identification of dimmers, which were proposed to be formed by direct union of two unoxidized triolein molecules. Because the ESI-MS spectra exhibited such abundant ammoniated molecules, we were able to identify at least two distinct types of unoxidized dimers. The peak at *m/z* 1785.6/1786.5 (all-^{12}C and first ^{13}C variant) arose from the combination of two triolein molecules *not* joined at the sites of unsaturation. One hydrogen was probably lost from each triolein molecule to form the bond at the site where they joined. Then, since the molecule had 114 carbons, the first ^{13}C isotope variant was more abundant than the all-^{12}C ammoniated molecule. This corresponds to the spectrum shown in Fig. 7(C), with *m/z* 1786.5 as the base peak. Immediately after this chromatographic peak, another dimer eluted that exhibited a mass spectrum in which the most abundant peaks (all-^{12}C and first ^{13}C variant) were at *m/z* 1787.4 and 1788.4 (spectrum not shown). This dimer was formed by joining the two triolein

RCM

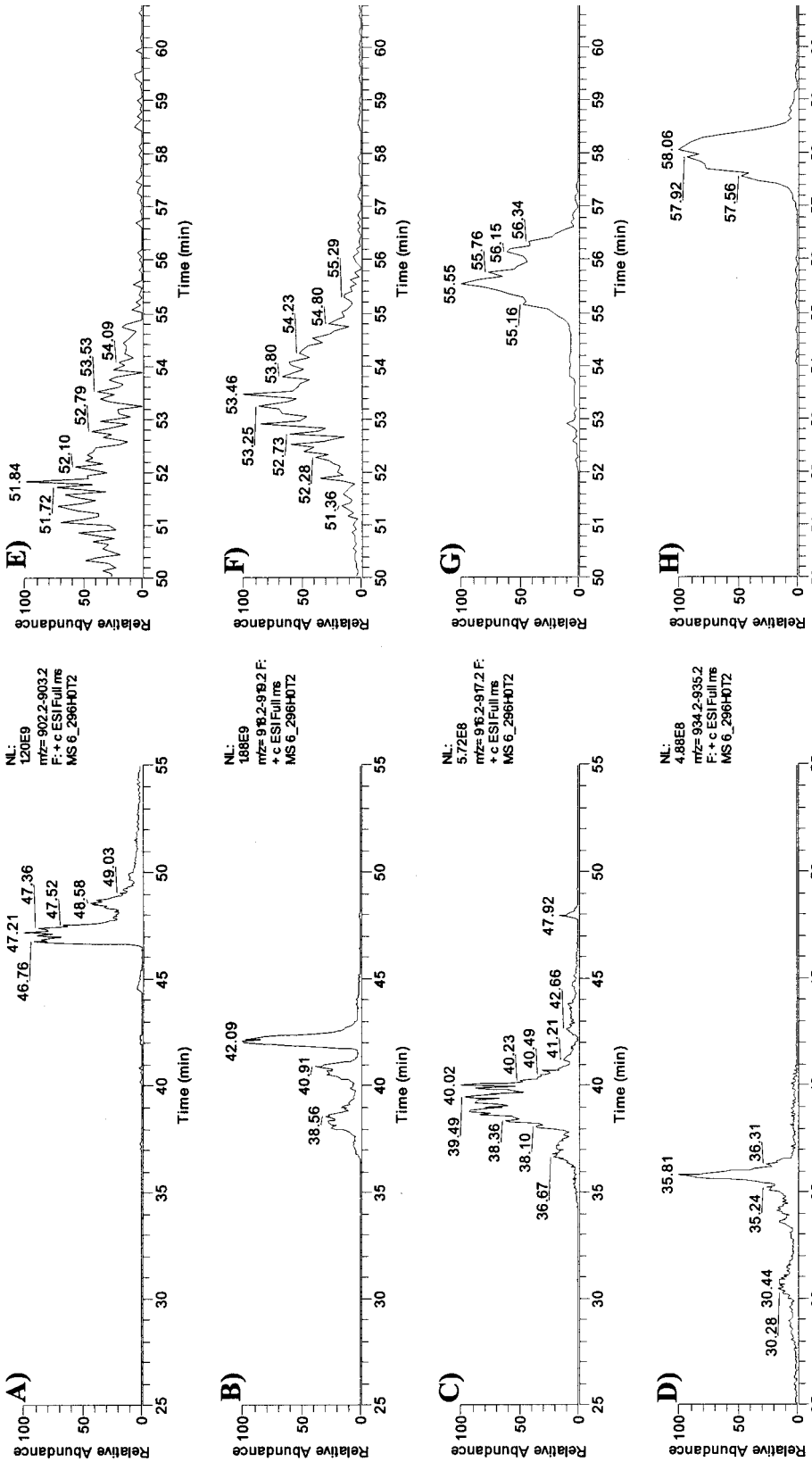

Figure 10. ESI-MS extracted ion chromatograms (EIC) showing triolein oxidation products. (A) EIC of ammoniated triolein, *m/z* 902.7; (B) EIC of ammoniated OOS-epoxide, keto-OOS and hydroxy-OOO, *m/z* 918.7; (C) EIC of ammoniated OOO-epoxide (multiple isomers), *m/z* 916.7; (D) EIC of ammoniated OOO-hydroperoxide, *m/z* 934.7; (E) EIC of ammoniated high molecular weight (MW) oxidized dimer containing four oxygen atoms, *m/z* 1851.1; (F) EIC of ammoniated high MW oxidized dimer containing three oxygen atoms, *m/z* 1835.2; (G) EIC of ammoniated high MW oxidized dimer with two oxygen atoms, *m/z* 1820.2; (H) EIC of ammoniated dimer with no additional oxygen atoms, *m/z* 1785.4.

molecules without the loss of the two additional hydrogen atoms. As expected, this molecule exhibited a slightly longer retention time because it contained one less site of unsaturation overall. The high sensitivity of ESI-MS to these large molecules via the formation of abundant intact ammoniated molecules will allow additional experiments to be performed to help elucidate the specific mechanisms of dimer formation. The mass spectrum in Fig. 7(C) also showed a fragment at *m/z* 902.7, corresponding to an ammoniated triolein moiety released from the dimer, as well as a diolein fragment ion at *m/z* 603.6.

The mass spectrum shown in Fig. 9(B) arose from a molecule containing two additional oxygen atoms on an oxidized dimer molecule (1787 + 32 = 1819). As with the unoxidized dimers, at least two types of these oxidized dimers were observed, with the later eluting one having an ammoniated molecule at *m/z* 1819, and the earlier eluting one having two fewer hydrogens, and so a *m/z* 1817 (1785 + 32 = 1817). The oxygen atoms on this molecule could either form the linkage between the two triolein molecules, or could be attached to the acyl chains of a carbon-linked dimer, e.g. a hydroperoxide of a dimer. Carbon-carbon versus carbon-oxygen-carbon linkages were mentioned in our previous work.[8] The mass spectrum showed that the molecule readily lost one oxygen atom through dehydration (producing ions at *m/z* 1801 and 1802 from *m/z* 1819 and 1820, respectively), but did not lose the second oxygen so readily. The fragment ions could simply be the ammoniated epoxide formed from a hydroperoxide.

Alternatively, the fragment ions could indicate that one oxygen atom formed a functional group that was readily lost, while the other oxygen was involved in the dimer linkage and so was not readily lost. It is hoped that further analysis and experiments using ESI-MS will provide data to help us further specify the exact natures of the linkages and functional groups involved. More extensive MS/MS and MS/MS/MS data than those demonstrated below will be required, targeted at specific molecular species, to provide additional clarification.

The retention time of the peak that eluted at 53.5 min indicates that this peak was more polar than the molecules discussed above. The *m/z* value of the corresponding ammoniated molecule indicates that the peak contained three oxygen atoms. A typical mass spectrum of these polar oxidized dimers is shown in Fig. 9(A). The trend of higher molecular weight oxidized dimers eluting before less polar dimers was previously observed by APCI-MS.[8] Smaller amounts of even more highly oxidized species eluted earlier than 53 min, and produced spectra showing larger ammoniated molecules (data not shown). The ESI-MS data provided excellent molecular weight information for the whole family of related oxygenated dimers, in contrast to APCI-MS spectra.

Lower molecular weight oxidation products

Extracted ion chromatograms of the base peaks in mass spectra shown in Figs 8 and 9 are shown in Fig. 10. Figure 10(A) shows the elution of intact triolein at 47 min, while Fig. 10(B) shows the EIC corresponding to the *m/z* value of ammoniated oxidized triolein containing one oxygen atom with no net loss of additional hydrogens. Ions at this *m/z* value included ammoniated hydroxy-OOO, keto-OOS, and OOS-epoxide (in which the epoxide formed across a double bond, as previously described[7,8]). OOS-epoxide was the largest peak in Fig. 10(B), while keto-OOS eluted just prior to OOS-epoxide (as we previously reported[8] by APCI-MS). Hydroxy-OOO appeared as the first peak in Fig. 10(B). TAGs containing hydroxyl groups produce little to no $[M + H]^+$ ions by APCI-MS,[15] but show abundant ammoniated molecule by ESI-MS under these conditions. Figure 10(C) shows the elution of OOO-epoxide, for which the EIC peak was broad due to the presence of multiple isomers, as we have shown by APCI-MS. Figure 10(D) shows the EIC of the *m/z* value corresponding to OOO-hydroperoxide, which is isobaric with epidioxy-OOS, if it were present. The sharpness of the peak in Fig. 10(D) rising out of the broader peak led us to believe that ESI-MS may provide direct evidence of intact epidioxy-OOS, where the epidioxy group is formed at a site of unsaturation in a triolein molecule. As with OOS-epoxide, the sharpness of the peak would be due to the fact that triolein had only one double bond across which the epidioxy group could form, so multiple isomers would not be possible. The abundance of the ammoniated molecule produced by ESI-MS allowed this peak to be observed, whereas it was not identified under APCI-MS conditions. On the other hand, APCI-MS spectra provided rich fragmentation that allowed other functional groups, such as the hydroperoxide group, to be identified. Figures 10(E)–10(H) represent high molecular weight dimers and oxidized dimers. Figure 10(H) corresponds to the EIC produced by the ammoniated molecule of the non-oxidized dimer formed by linkage not at a double bond, for which the mass spectrum was shown in Fig. 9C. Figure 10(G) shows the EIC of the ammoniated dimer containing two oxygen atoms; Fig. 10(F) represents the dimers containing three oxygen atoms; and Fig. 10(E) represents those dimers containing four oxygen atoms. These EICs confirmed that the molecules eluted in the order of most oxygen atoms (and therefore most polar) eluted first, followed by those with fewer oxygen atoms (and therefore least polar) last.

We have previously used APCI-MS to identify chain-shortened oxidation products, in which a part of a triolein chain was lost. Using ESI-MS we have now been able to observe ammoniated molecules for two types of chain-shortened products. Figure 11 shows extracted ion chromatograms of masses corresponding to several of these chain-shortened products. Between 32 and 40 min, molecular species are present having $[M + NH_4]^+$ ions at *m/z* 722.6, 736.6, 750.6, 764.6, 778.5 and 790.5, representing losses of 8, 9, 10, 11, 12, and 13 carbon fragments, respectively. These species appear to represent chain-shortened TAGs in which any oxygen functional groups were lost in the leaving fragment. The most abundant species had an $[M + NH_4]^+$ at *m/z* 764.5, as shown in Fig. 11(F). This *m/z* value corresponded to the TAG left when a triolein chain broke between carbons 8 and 9, leaving a $O_2C_8H_{15}$ acyl chain fragment on the TAG. The least abundant species was observed at *m/z* 778.6 (Fig. 11(E)) which corresponded to the species formed by fragmentation between carbons 9 and 10, the location of the double bond. Another set of chain-shortened TAGs

RCM

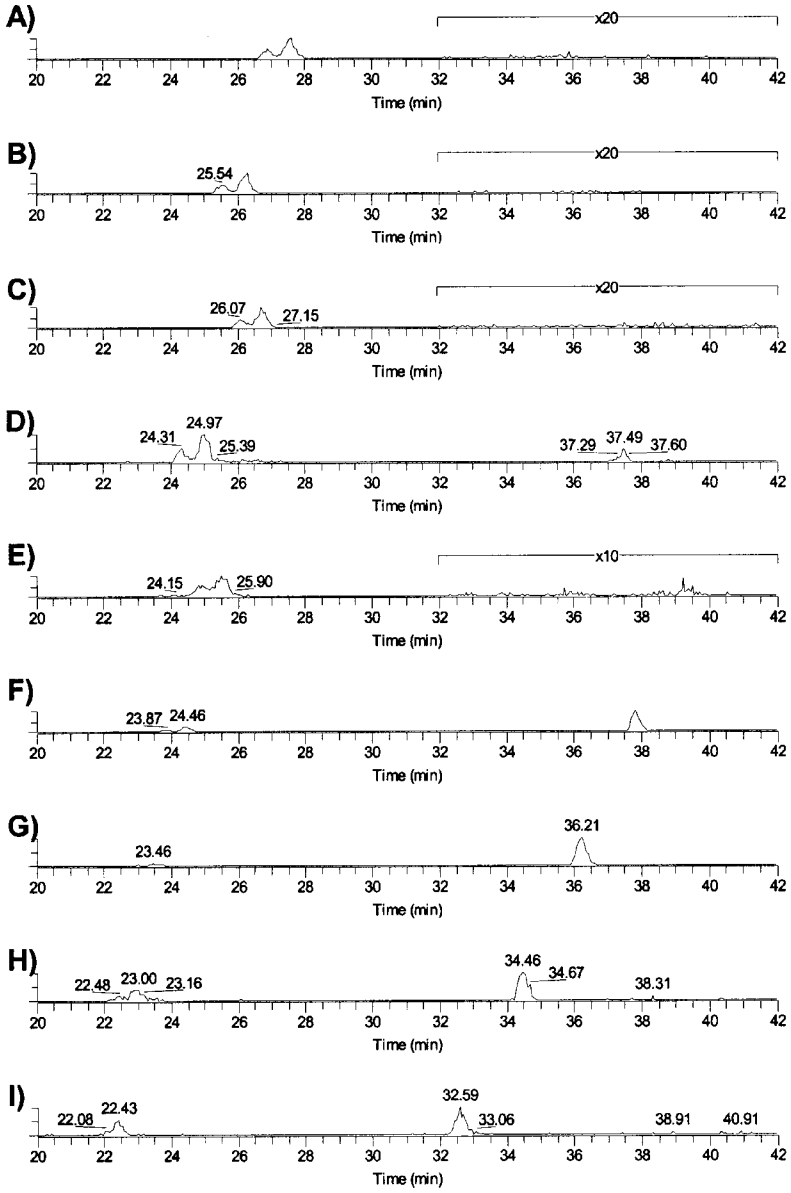

Figure 11. Extracted ion chromatograms of core aldehydes (or epoxides) and chain-shortened TAG. (A) EIC of *m/z* 818.7, = OO,$C_{11}H_{17}O_3$; (B) EIC of *m/z* 804.7, = OO,$C_{10}H_{15}O_3$; (C) EIC of *m/z* 792.7, = OO,$C_9H_{15}O_3$; (D) EIC of *m/z* 790.7, = OO,$C_9H_{13}O_3$ & = OO,$C_{10}H_{17}O_2$; (E) EIC of *m/z* 778.7, = OO,$C_8H_{13}O_3$ & = OO,$C_9H_{17}O_2$; (F) EIC of *m/z* 764.6, = OO,$C_7H_{11}O_3$ & = OO,$C_8H_{15}O_2$; (G) EIC of *m/z* 750.7, = OO,$C_6H_9O_3$ & = $C_7H_{13}O_2$; (H) EIC of *m/z* 736.6, = OO,$C_5H_7O_3$ & = OO,$C_6H_{11}O_2$; (I) EIC of *m/z* 722.6, = OO,$C_4H_5O_3$ & = OO,$C_5H_9O_2$.

eluted between 22 and 28 min. These had many of the same *m/z* values as the later eluted chain-shortened TAGs, but the retention times of the earlier eluted species indicate increased polarity compared to the later eluted species. The earlier species appear to represent chain-shortened species in which an oxygen functional group remained on the TAG. These molecules could be either core aldehydes or epoxides. These two classes are isobaric and the fragmentation patterns of these chain-shortened polar components did not allow us to differentiate them. In the mass spectra of all of these components, an abundant fragment at *m/z* 603.5, representing diolein, indicates that the oxygen functional group was on the chain-shortened acyl chain. The most abundant of these molecular species was that having an ammoniated molecule at *m/z* 804.7, which corresponded to loss of a C_8 chain, leaving an intact $O_2C_{10}H_{15}O$ chain fragment (either a core aldehyde or epoxide).

We also previously used APCI-MS to report the presence of chain-branched addition products,[8] in which molecular fragments added onto intact triolein. We were only able to observe these components by APCI-MS of an enriched sample after preparative HPLC of high molecular weight

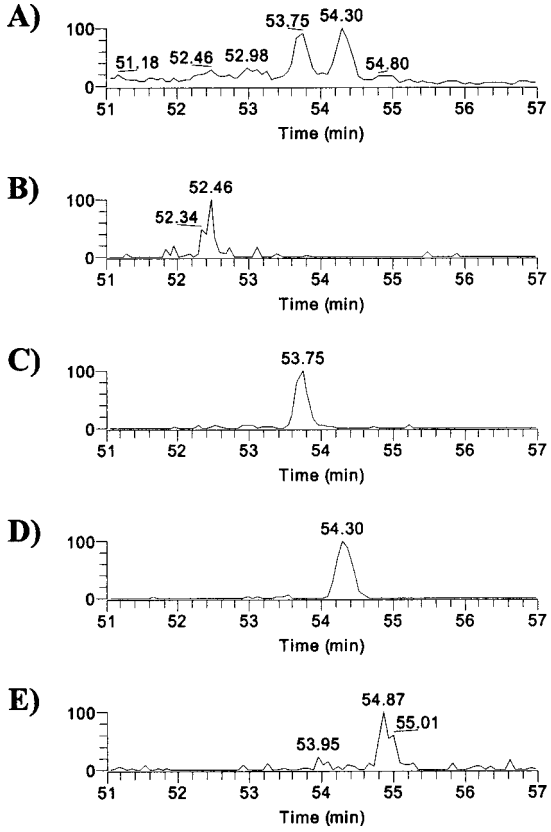

Figure 12. Extracted ion chromatograms (EIC) of ammoniated chain-addition products of heated triolein by ESI-MS. (A) EIC of *m/z* range 970-1040; (B) EIC of *m/z* 974.7, = OOO − H + OC_4H_9; (C) EIC of *m/z* 1002.7, = OOO − H + OC_6H_{13}; (D) EIC of *m/z* 1016.7, = OOO − H + OC_7H_{15}; (E) EIC of *m/z* 1030.7, = OOO − H + OC_8H_{17}. Compare to Fig. 8, Ref. 8.

components. In contrast, ESI-MS allowed these components to be observed in the original sample with no enrichment required. Figure 12 shows extracted ion chromatograms of the $[M + NH_4]^+$ ions corresponding to the same chain-branched addition products which we previously reported by APCI-MS (Fig. 8 in Ref. 8). The only addition product that was not observed in this sample was the one which had given a fragment at *m/z* 689.6 in the previous report. These chain-branched addition products were not evident in the total ion chromatogram because they occurred overlapped with polar dimer products. However, extracting out the mass range of these species in the form of an EIC allowed these chain-addition products to be readily identified.

MS/MS and MS^3 data

The intact $[M + NH_4]^+$ ions exhibited by ESI-MS were a valuable complement to the fragments produced by APCI-MS, but we further sought to perform MS/MS and MS/MS/MS to observe how such spectra compared to the fragments produced by APCI-MS. ESI-MS, ESI-MS/MS and ESI-MS/MS/MS spectra of triolein oxidation products are shown in Fig. 13. Figure 13(A) shows the EIC of OOO + 16, which resulted either from addition of an oxygen at the site of unsaturation, or replacement of a hydrogen with a hydroxy group, as in Fig. 10(B). An EIC constructed from all MS/MS scans having *m/z* 918.7 as the precursor ion is shown in Fig. 13(B). An EIC of all MS/MS/MS scans which had *m/z* 918.7 as the precursor ion and *m/z* 619.5 as the first-generation product (daughter) ion, to produce granddaughter ions, is shown in Fig. 13(C). The averaged mass spectrum across the largest peak in the EIC of *m/z* 918.7 (Fig. 13(A)) is shown in Fig. 13(D), which corresponds to Fig. 8(A). As mentioned, several oxidation products had a *m/z* value of 918.7. Average MS/MS spectra of the two largest peaks from Fig. 13(B) are shown in Figs 13(E) and 13(F). The retention of the first peak, relative to the second peak (which has been shown to be OOS-epoxide), specified the first peak as keto-OOS, as we previously reported.[8] The ESI-MS/MS spectrum of keto-OOS was highly similar to the mass spectrum obtained by using APCI-MS reported earlier (Fig. 3(B) in Ref. 8). Likewise, the ESI-MS/MS spectrum of OOS-epoxide in Fig. 13(F) was very similar to the mass spectrum of this molecule reported earlier by APCI-MS. The fragmentation mechanism of a species containing an oxygen at, not next to, a double bond, is the same in this ESI-MS/MS spectrum as we previously reported by APCI-MS.[7] The fragment ratios in the ESI-MS/MS spectra were very similar to those seen in APCI-MS spectra. Further fragmentation of the *m/z* 619.5 daughter ions yielded the MS/MS/MS spectra shown in Figs 13(G) and 13(H). An important difference between these MS/MS/MS spectra is the size of the peak at *m/z* 601.4, which was equivalent to $[OL]^+$. This fragment was completely consistent with the fragmentation mechanism described previously[7] for an epoxide ring formed not next to a double bond, showing that ESI-MS/MS/MS also followed the same mechanism. It was observed in the MS/MS and MS/MS/MS spectra that ammoniated species were not present, and only protonated or even-electron fragment ions appeared in the ESI-MS/MS and MS/MS/MS spectra.

ESI-MS, ESI-MS/MS and ESI-MS/MS/MS spectra of high molecular weight triolein oxidation products are shown in Fig. 14. An MS^n isolation width of 2 *m/z* units allowed the all-^{12}C and first isotope variant peaks to be investigated together. In Fig. 14(A), the ion at *m/z* 1819.2 was that expected to arise from an ammoniated triolein dimer which contained a hydroperoxide group, or $2 \times (OOO) - H + OOH + NH_4$, or $2 \times 884.8 + 32 + 18 = 1819.6$. Again, the isotope peak at *m/z* 1820 was larger than the *m/z* 1819 peak, because of the large number of carbon atoms. The ion at *m/z* 1801 then represented the ammoniated epoxide formed from loss of 18 Da from the ammoniated hydroperoxide dimer (1819 − 18 = 1801, or 1820 − 18 = 1802). Then, in the ESI-MS/MS spectrum in Fig. 14(B), the *m/z* 1767 peak represented the protonated (protonated, not ammoniated fragments appeared in MS/MS spectra, as in Fig. 13) dimer after loss of the epoxide group: $1802.3 - H_2O - NH_4 + H = 1767.3$. This implied loss of the epoxide by a mechanism such as that previously described,[7] which resulted in a net loss of H_2O, indicating that the epoxide was next to a double bond. The ion at *m/z* 1503.2 was consistent with the loss of one oleoyl acyl chain (= 281.3 Da) from the *m/z* 1802 epoxide precursor, and further loss of ammonium, 1802 − 281 − 18 = 1503. Note that loss of one oleoyl fatty chain formed an

RCM

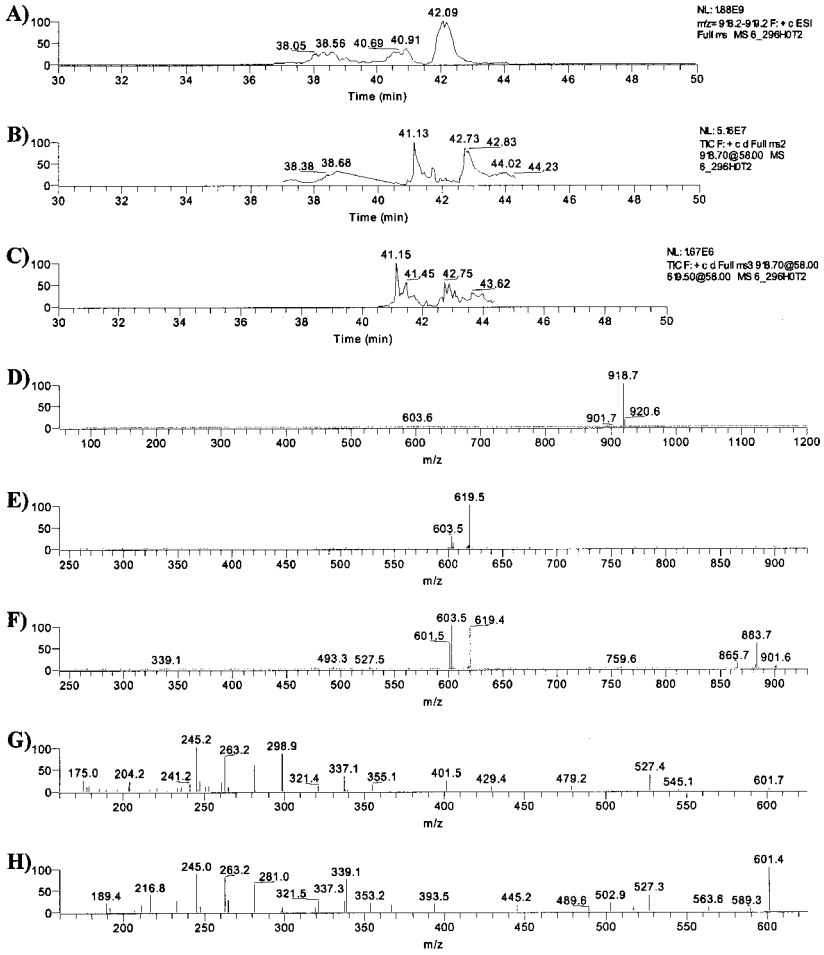

Figure 13. ESI-MS, ESI-MS/MS and ESI-MS/MS/MS Spectra of triolein oxidation products. (A) EIC of *m/z* 918.7; (B) EIC of all MS/MS scans of *m/z* 918.7; (C) EIC of all MS/MS/MS scans of *m/z* 619.5; (D) Mass spectrum averaged across peak at 42 min; (E) MS/MS spectrum averaged across peak at 41.1 min in (B), = keto-OOS; (F) MS/MS spectrum averaged across peak at 42.7 min in (B), = epoxy-OOS; (G) Average MS/MS/MS spectrum of keto-OOS; (H) Average MS/MS/MS spectrum of epoxy-OOS.

ion without the need for a proton to provide an ionic charge, exactly as a diacylglycerol fragment ion formed by loss of a FA chain from a TAG is not protonated in APCI-MS spectra (e.g. $-[OOO + H]^+ - RCOO - H$: $885.8 - 281.3 - 1 = 603.5$). This fragment then still contained an epoxide which was also lost to form the *m/z* 1485 peak.

The case of the non-oxygenated dimer was more straightforward. An ammoniated triolein dimer at *m/z* 1786.5 was apparent in the mass spectrum in Fig. 14(D). The ESI-MS/MS spectrum of this molecule in Fig. 14(E) showed the loss of an oleoyl acyl chain (and the ammonium ion), or $1786 - 281 - 18 = 1487$ (and $1785 - 281 - 18 = 1486$). Again, when an oleoyl chain was lost, a proton was not necessary to form an ion on the remaining molecular fragment, just as with fragmentation of a TAG. Other MS/MS and MS/MS/MS fragments await further characterization. It was apparent from these data that ESI-MS/MS and MS/MS/MS data provide valuable information to allow the identities of high molecular weight oxidation products to be determined.

TAG positional isomers

It has been reported that the location of the fatty acyl chain on the glycerol backbone affected the fragmentation pattern of TAG analyzed by APCI-MS.[4–6] The loss of the fatty acyl chain in the *sn*-2 position has been reported to be energetically disfavored. We sought to determine whether similar trends were observed under these ESI-MS conditions. Figure 15 shows ESI-MS, ESI-MS/MS, ESI-MS/MS/MS, APCI-MS and APCI-MS/MS spectra of OPO and POP. As was observed for TAG in canola oil, the ESI-MS spectra exhibited primarily $[M + NH_4]^+$ ions, with small abundances of DAG fragment ions. As mentioned above, the ESI-MS/MS product ion mass spectra were very similar to the APCI-MS spectra. Figure 15(B) is very similar to Fig. 15(G), and Fig. 15(E) is very similar to Fig. 15(I). The small abundances of fragments at *m/z* 603.5 (=$[OO]^+$) in Fig. 15(B) and *m/z* 551.5 (=$[PP]^+$) in Fig. 15(E), compared to the peak at *m/z* 577.5, indicates that there was discrimination in ESI-MS/MS spectra based on the position of the fatty acids

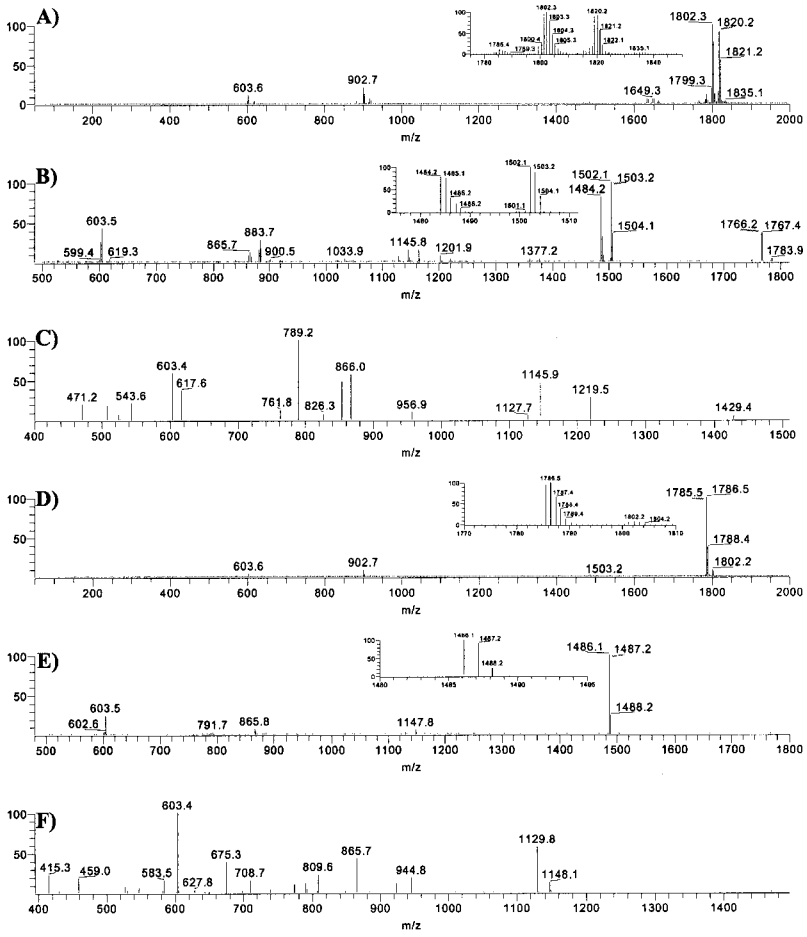

Figure 14. ESI-MS, ESI-MS/MS and ESI-MS/MS/MS spectra of high molecular weight triolein oxidation products. (A) ESI-MS spectrum of peak eluted at 55–57 min in Fig. 10(F); (B) MS/MS of *m/z* 1802.4; (C) MS/MS/MS of *m/z* 1502.1; (D) ESI-MS spectrum of peak eluted at 58 min in Fig. 10(G); (E) MS/MS of *m/z* 1786.5; (F) MS/MS/MS of *m/z* 1486.1.

on the glycerol backbone. Statistically, the combination of 1,2- and 2,3-DAG fragment ions of OPO and POP should be present in a ratio of 2:1 compared to the 1,3-DAG fragment ions. In the spectra in Figs 15(B) and 15(E), the abundance of the 1,3-DAG fragment was substantially lower than half that of the base peak, indicating that the 1,3-DAG fragment was energetically disfavored. Tables 2 and 3 list the abundances of the fragment ions which arose from five positional isomers analyzed for this report.

These data indicated that the 1,3-isomers were energetically disfavored, and produced a lower than statistically predicted abundance (<50%) compared to the combined 1,2- and 2,3-DAG fragments, as has been observed in APCI-MS spectra.[4,5] It was expected that this trend might carry over into the ESI-MS/MS/MS spectra, but this was not the case. The *m/z* 577.4 peak in Fig. 15(B) represented the combined 1,2- and 2,3-fragments $[OP]^+$ and $[PO]^+$. If the fatty acyl chain was lost from the 1- or 3-position preferentially, it would be expected that the $[RCO]^+$ fragment would be from the fatty acyl chain in the 1- and 3-positions, while the $[RCOO + 58]^+$ ion would preferentially represent the fatty acyl chain in the 2-position. Figure 15(C) appeared to obey this behavior, with the largest $[RCO]^+$ peak at *m/z* 265.2 (=$[C_{18}H_{33}O]^+$), and the largest $[RCOO + 58]^+$ peak at *m/z* 313.2 (=$[C_{16}H_{31}O + 58]^+$). However, comparison of Figs 15(F) and 15(C) showed that POP produced almost the same abundances of $[RCO]^+$ fragment ions, even though the 'P' acyl chains were in both the 1- and 3-positions in this molecule. In Fig. 15(F), the $[RCOO + 58]^+$ ion abundances were small. The ESI-MS/MS/MS spectra of OOP and PPO (not shown) were also very similar to the mass spectra in Fig. 15. The position of the fatty acyl chain appeared to have little effect on the fragment ratios in the ESI-MS/MS/MS spectra. The stability of the fragment ion itself appeared to be the determining factor in the abundances of the fragment ions produced. The monounsaturated oleoyl chain formed a more stable $[RCO]^+$ fragment ion than the palmitic acyl chains. Conversely, in most ESI-MS/MS/MS spectra, the $[RCOO + 58]^+$ fragment ion formed from palmitic acid was more abundant than that formed from the oleoyl acyl chain. The $[RCO]^+$ fragment ions in the APCI-MS/MS spectra in Figs 15(H) and 15(J), on the other hand, did reflect the position of the fatty acyl chain, but in a manner that was opposite to that of the expected trend. The fatty acid in the 2-

RCM

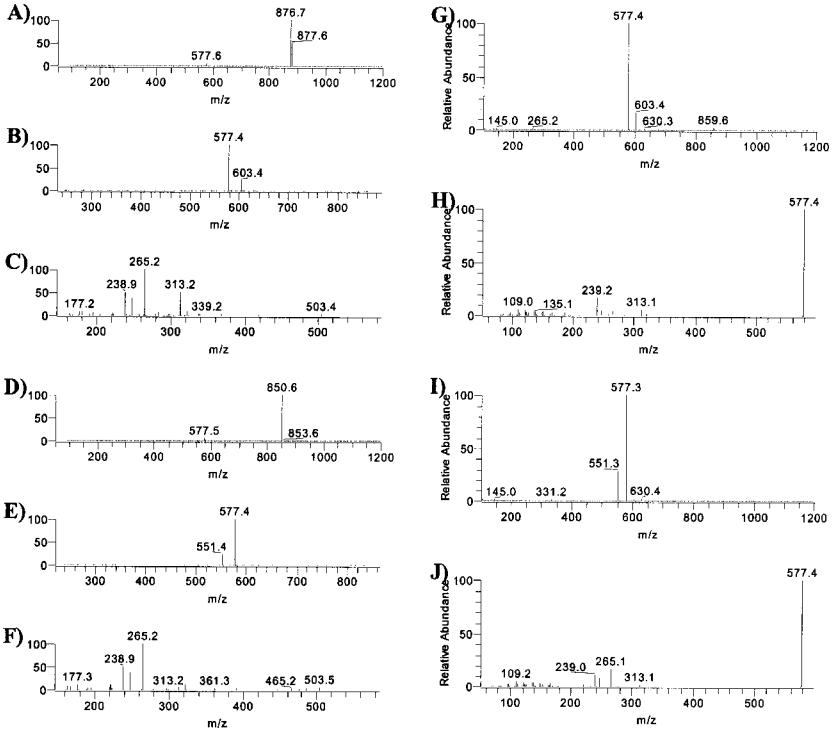

Figure 15. ESI-MS, ESI-MS/MS, ESI-MS/MS/MS, APCI-MS and APCI-MS/MS spectra of TAG positional isomers. (A) ESI-MS spectrum of OPO; (B) ESI-MS/MS spectrum of *m/z* 876.7; (C) ESI-MS/MS/MS spectrum of *m/z* 577.4; (D) ESI-MS of POP; (E) ESI-MS/MS spectrum of *m/z* 850.8; (F) ESI-MS/MS/MS of *m/z* 577.4; (G) APCI-MS spectrum of OPO; (H) APCI-MS/MS spectrum of *m/z* 577.4; (I) APCI-MS spectrum of POP; (J) APCI-MS/MS spectrum of *m/z* 577.4.

Table 2. DAG fragment ion abundances by ESI-MS

	[OO]+	[OP]+	[PP]+	[OS]+
OPO	24.4	100.0		
OOP	67.7	100.0		
POP		100.0	23.3	
PPO		100.0	67.7	
OOS	63.7			100.0

Table 3. DAG fragment ion abundances by APCI-MS

	[OO]+	[OP]+	[PP]+	[OS]+
OPO	16.7	100.0		
OOP	50.7	100.0		
POP		100.0	29.3	
PPO		100.0	87.4	
OOS	53.9			100.0

position actually produced the larger abundance of the $[RCO]^+$ fragment ion.

CONCLUSIONS

ESI-MS and APCI-MS produced complementary data. The ESI-MS approach employed a conventional separation, but with a sheath liquid added to supply electrolyte. The ESI produced abundant and reproducible ammoniated molecules from normal triacylglycerols, triacylglycerol oxidation products, and from high molecular weight TAG dimers and oxidized dimers. These ammonium adducts allowed the molecular weights of the molecules to be readily determined. Intact ionized molecules other than the ammoniated adduct were not produced by ESI. Small but sufficient levels of DAG fragment ion abundances were produced in ESI-MS spectra to allow the use of extracted ion chromatograms to assist in identification of molecular species. ESI-MS was more sensitive than APCI-MS to all TAGs, and was more sensitive to polyunsaturated TAGs than to saturated TAGs. This was opposite to the trend in APCI-MS spectra, in which saturated TAGs gave higher sensitivity. ESI-MS spectra showed abundant $[M + NH_4]^+$ ions for intact molecules that produced little or no $[M + H]^+$ ions under APCI-MS conditions, such as hydroxy-, keto- and hydroperoxy-TAGs. In fact, ESI-MS was more sensitive to triolein oxidation products than to triolein itself. The ability of ESI-MS to produce intact $[M + NH_4]^+$ ions of high molecular weight oxidized and non-oxidized dimers allowed these compounds to be identified without the need for sample collection and enrichment.

The tendency of APCI-MS to form $[M + H]^+$ ions plus structurally diagnostic fragment ions was very beneficial. The mass spectra produced by APCI-MS provided an added degree of confidence in the assignment of molecular weights until we had gained sufficient confidence that ESI-MS

spectra contained only ammoniated molecules, with no other molecular adduct ions which would complicate interpretation. Product ion mass spectra produced by ESI-MS/MS were very similar in appearance to conventional APCI-MS spectra. Like APCI-MS, ESI-MS/MS spectra allowed identification of positional isomers based on the ratios of diacylglycerol fragment ions. Loss of fatty acyl chains from the 1- and 3-positions was favored in ESI-MS/MS spectra. On the other hand, we have not yet correlated fragment ions produced by ESI-MS/MS/MS to the positional placement of the fatty acyl chains. The identities of the fatty acyl chains themselves, rather than their placement, had a greater impact on the abundances of the fragment ions produced in ESI-MS/MS/MS spectra. Conversely, fragment ions were observed in APCI-MS/MS spectra that appeared to correlate to the position of the fatty acyl chains. Polyunsaturated TAGs exhibited higher levels of charge-remote fragmentation than did highly saturated TAGs.

The dual parallel mass spectrometer approach produced identical retention times in the ESI-MS and APCI-MS spectra, allowing unambiguous comparison between the mass spectra obtained by both techniques. Because of the very different appearances of the chromatograms obtained under ESI versus APCI conditions, it would be harder to compare TAG peaks in chromatograms from ESI-MS to APCI-MS without the identical retention times made possible by the dual parallel arrangement. The dual parallel mass spectrometer approach produced a wealth of information to allow numerous classes of TAG and TAG oxidation products to be determined, it saved time, conserved solvent and sample, and saved wear on columns and LC instruments by obtaining data from two mass spectrometers simultaneously instead of sequentially.

REFERENCES

1. Byrdwell WC, Emken EA. *Lipids* 1995; **30**: 173.
2. Byrdwell WC, Emken EA, Neff WE, Adlof RO. *Lipids* 1996; **31**: 919.
3. Byrdwell WC, Neff WE. Qualitative and Quantitative Analysis of Triacylglycerols Using Atmospheric Pressure Chemical Ionization Mass Spectrometry, In *New Techniques and Applications in Lipid Analysis*, McDonald RE, Mossoba MM (eds). AOCS Press: Champaign, IL, 1997; 45–80.
4. Laakso P, Voutilainen P. *Lipids* 1996; **31**: 1311.
5. Mottram HR, Evershed RP. *Tetrahedron Lett.* 1996; **37**: 8593.
6. Mottram HR, Woodbury SE, Evershed RP. *Rapid Commun. Mass Spectrom.* 1997; **11**: 1240.
7. Neff WE, Byrdwell WC. *J. Chromatogr. A* 1998; **818**: 169.
8. Byrdwell WC, Neff WE. *J. Chromatogr. A* 1999; **852**: 417.
9. Byrdwell WC, Neff WE. *J. Chromatogr. A* 2001; **905**: 85.
10. Byrdwell WC. *Lipids* 2001; **36**: 327.
11. Manninen P, Laakso P. *J. Am. Oil Chem. Soc.* 1997; **74**: 1089.
12. Mochida Y, Yokoyama Y, Nakamura S. *J. Mass Spectrom. Soc. Jpn* 1998; **46**, 246.
13. Byrdwell WC. *Rapid Commun. Mass Spectrom.* 1998; **12**: 256.
14. Ikeda M, Kusaka T. *J. Chromatogr.* 1992; **575**: 197.
15. Byrdwell WC, Neff WE. *J. Liq. Chromatogr. Related Technol.* 1998; **21**: 1485.
16. Mu H, Sillen H, Hoy CE. *J. Am. Oil Chem. Soc.* 2000; **77**: 1049.
17. Adas F, Picart D, Berthou F, Simon B, Amet Y. *J. Chromatogr. B* 1998; **714**: 133.
18. Kusaka T, Ishara S, Sakaida M, Mifune A, Nakan Y, Tsuda K, Ikeda M, Nakano H. *J. Chromatogr. A* 1996; **730**: 1.
19. Duffin KL, Henion JD, Shieh JJ. *Anal. Chem.* 1991; **63**: 1781.
20. Myher JJ, Kuksis A, Geher K, Park PW, Diersen-Schede DA. *Lipids* 1996; **31**: 207.
21. Sandra P, Dermaux A, Ferraz V, Dittman MM, Rozing G. *J. Micro. Sep.* 1997; **9**: 409.
22. Sjovall O, Kuksis A, Marai L, Myher J. *Lipids* 1997; **32**: 1211.
23. Cheng C, Gross ML, Pittenauer E. *Anal. Chem.* 1998; **70**: 4417.
24. Schuyl PJW, de Joode T, Vasconcellos MA, Duchateau GSMJE. *J. Chromatogr. A* 1998; **810**: 53.
25. Hsu FF, Turk J. *J. Am. Soc. Mass Spectrom.* 1999; **10**: 587.
26. Han X, Abendschein DR, Kelley JG, Gross RW. *Biochem. J.* 2000; **352**: 79.
27. Han X and Gross RW. *Anal. Biochem.* 2001; **295**: 88.
28. Dermaux A, Medvedovici A, Ksir M, Van Hove E, Talbi M, Sandra P. *J. Micro. Sep.* 1999; **11**: 451.
29. Steenhorst-Slikkerveer L, Louter A, Janssen HG, Bauer-Plank C. *J. Am. Oil Chem. Soc.* 2000; **77**: 837.
30. Endo Y, Tagiri-Endo M, Seo HS, Fujimoto K. *J. Chromatogr. A* 2001; **911**: 39.
31. Hvattum E. *Rapid Commun. Mass Spectrom.* 2001; **15**: 187.
32. Siegel MM, Tabei K, Lambert F, Candela L, Zoltan B. *J. Am. Soc. Mass Spectrom.* 1998; **9**: 1196.
33. Byrdwell WC, Neff WE. *J. Liq. Chromatogr. Related Technol.* 1996; **19**: 2203.
34. Byrdwell WC, Neff WE, List GR. *J. Agric. Food Chem.* 2001; **49**: 446.
35. Neff WE, List GR, Byrdwell WC. *J. Liq. Chromatogr. Related Technol.* 1999; **22**: 1649.
36. Shibayama N, Lomax SQ, Sutherland K, de la Rie ER. *Stud. Conserv.* 1999; **44**: 253.
37. Holcapek M, Jandera P, Fischer J, Prokes B. *J. Chromatogr. A* 1999; **858**: 13.
38. Valeur A, Michelsen P, Odham G. *Lipids* 1993; **28**: 255.
39. Aasen AJ, Lauer WM, Holman RT. *Lipids* 1973; **5**: 869.
40. Lauer WM, Aasen AJ, Graff G, Holman RT. *Lipids* 1973; **5**: 861.